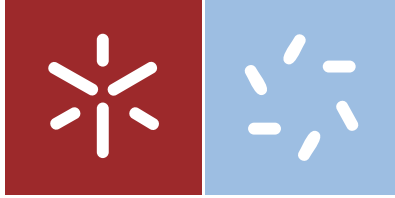


Universidade do Minho
Escola de Ciências

João Alberto Cunha Barbosa

Development of a poly(L-Lactic acid) based
drug release system.



Universidade do Minho
Escola de Ciências

João Alberto Cunha Barbosa

Development of a poly(L-Lactic acid) based
drug release system.

Dissertação de Mestrado
Mestrado em Biofísica e Bionanossistemas

Trabalho realizado sob a orientação do
Professor Doutor Senentxu Lãnceros-Mendez
Doutora Clárisse Ribeiro

DECLARAÇÃO

Nome: João Alberto Cunha Barbosa

Endereço eletrónico: joaoa.c.barb@gmailcom **Telefone:** 919770948

Cartão do Cidadão: 13619060

Título da dissertação: Development of a poly(L-Lactic acid) based drug release system (Desenvolvimento de um sistema de libertação de fármacos baseado no ácido poli(L-láctico)).

Orientadores:

Professor Doutor Senentxu Lanceros-Mendez

Doutora Clárisse Ribeiro

Ano de conclusão: 2015

Mestrado em Biofísica e Bionanossistemas

É AUTORIZADA A REPRODUÇÃO INTEGRAL DESTA DISSERTAÇÃO APENAS PARA EFEITOS DE INVESTIGAÇÃO, MEDIANTE DECLARAÇÃO ESCRITA DO INTERESSADO, QUE A TAL SE COMPROMETE.

Universidade do Minho, ____/____/____

Assinatura:

AKNOWLEDGMENTS

I would like to greatly thank Professor Senentxu Lanceros-Mendez, my supervisor, for always being present, for all the advices, for all the guidance and also for all the support in all stages of my thesis, since my integration in the group until the final step to conclude this journey. Thank you for everything, your leadership is truly inspiring...

I am also grateful to both my co-supervisors, Vitor Sencadas and Clarisse Ribeiro. It was a pleasure to work with Vitor and learn from his great experience and ideas, even though it was for a short time. Also, thank you Clarisse for all the support. Even though you were not working directly with me since the begging of my thesis, you were always available to help any way you could.

I would also like to thank Professor Paul Cox, from University of Portsmouth, for all his help and hospitality during my Erasmus exchange.

A special big thank you to Daniela Correia. Firstly, for you unconditional support in every single moment. Even when you were struggling to do your own work, you always tried to find time to help me as well. You were honestly a fantastic help and a great company. Also, a thank you to Renato Gonçalves, that alongside Daniela helped me to perform part of my experiments when I was abroad and was always ready to help.

A warm thank you to all the ESM group for continuously integrating new members the best way you can and for the great work environment you all create. I never felt left out when I was working there. Thank you all for always being available to help when I needed something.

To my closest friends who sometimes had to deal with my bad mood and my crisis due to this master, thank you. A special word to Diana Leite, who is still the only friend that truly understands what I do and with whom I can discuss my work and my problems – thank you so much for still being there for me!

Finally, a singular thank you and apologies to my parents and sister. Thank you for the support, for trying to understand why I spend so much time working, for letting me pursue my dream and create the possibilities for me to keep studying. You always were, and are, a safe harbor, a place of calm.

Thank you to all people who, in some way, helped me and contributed to my success during this journey. As Jim Morrison put it “There are things known and things unknown; between them are only doors” – It is now time for me to open a new door...

RESUMO

A nanomedicina e os sistemas de entrega controlada de fármacos iniciaram recentemente a sua utilização terapêutica. Várias práticas utilizadas pela medicina convencional apresentam diversas limitações e são, muitas vezes, ineficazes, sendo necessária a sua substituição por novos materiais que assegurem que um fármaco é entregue no local certo, no momento adequado. Apesar de vários materiais poliméricos serem já utilizados para produzir sistemas de entrega de fármacos com características moduláveis é no entanto necessário ter um controlo ativo da taxa de libertação. Assim, a adição de um componente sensível a um estímulo que pudesse iniciar ou acelerar a libertação seria uma grande vantagem. Deste modo, neste trabalho foi desenvolvida uma plataforma polimérica contendo um veículo no qual o fármaco está integrado (zeólito) e um componente sensível a campos magnéticos (Terfenol-D).

Inicialmente, foi realizado um estudo teórico e experimental envolvendo diversos zeólitos com diferentes características (estrutura, tamanho do cristal, razão Si/Al e contra-íão) e métodos de incorporação do fármaco usando diferentes solventes (hexano, etanol e acetona), de maneira a entender a influência dos diferentes parâmetros na incorporação de um fármaco modelo – ibuprofeno. Seguidamente, foi otimizada a preparação das membranas de ácido poli(L-láctico) para a incorporação dos restantes componentes, tendo sido testadas quatro concentrações de polímero.

Os resultados demonstraram que as estruturas faujasite e *beta polymorph-a* foram as que apresentaram maior mobilidade para a molécula do fármaco e o hexano mostrou ser o solvente que permite maiores taxas de encapsulação. Dos zeólitos testados, foi selecionado o que apresentava libertação total do seu conteúdo às 24h (faujasite com tamanho de cristal de ~250nm). Os testes às membranas mostraram que a membrana com 5 (m/vol.)% de polímero apresentava as características morfológicas e mecânicas mais adequadas, mantendo-as após a incorporação do zeólito e das partículas de Terfenol-D

Comparando as cinéticas de libertação dos quatro sistemas de libertação preparados (zeólitos e membranas carregados; membranas com zeólitos carregados; e membranas com zeólitos carregados e Terfenol-D sob campos magnéticos) claras diferenças são observadas. A libertação de IBU das membranas contendo zeólitos carregados aparenta ser uma combinação das cinéticas de libertação dos zeólitos e das membranas carregados. Os ensaios de libertação com as membranas contendo zeólito e Terfenol-D sob campos magnéticos confirmaram a influência do estímulo na taxa de libertação. O resultado foi um transporte denominado super caso-II, indicando que o mecanismo de libertação é controlado sobretudo pelas variações na matriz polimérica, causada pelo movimento das partículas magnetostriativas.

Palavras-Chave: Zeólitos, ácido poli(L-láctico), modelação molecular, libertação controlada, estímulo magnético

ABSTRACT

Nanomedicine and controllable drug delivery systems have recently initiated their way into therapeutics. Faulty and, many times, ineffective approaches that conventional medicine uses need to be replaced by novel and smart materials that assure that a drug is delivered in the right place, at the right time. Polymeric materials are now widely used to produce drug delivery vehicles with tunable characteristics and, if needed, triggered releases. Although several polymeric materials are already being used to produce drug delivery systems it is, however, necessary to reach an active control of the drug release rate. Hence, the addition of a stimuli-sensitive component to the system that could trigger or increase the drug release rate would be of great interest. Therefore, during this work a polymeric platform containing a drug carrier (zeolite) and a stimuli-sensitive component (Terfenol-D) was developed.

Firstly, a theoretical and experimental screening involving different zeolites with different characteristics (structure, crystal size, Si/Al ratio and counter ion) and loading methods with different solvents (hexane, ethanol and acetone) was performed in order to understand their influence in the loading of a model drug – Ibuprofen. Next, preparation of poly(L-lactic acid) membranes was optimized by testing three different polymer concentration. The membranes were prepared by freeze-drying method.

Preliminary results from the molecular modelling studies indicated that faujasite and beta polymorph-A structures were the ones allowing a greater displacement of the drug inside the pores. Experimental trials indicated that hexane was the solvent providing greater loadings. From the tested zeolites, the nanosized faujasite (crystal size of ~250nm) was selected due to its complete drug release at 24h. Moreover, membranes prepared with 5(wt/vol.)% presented the best morphological and mechanical characteristics that were maintained after the incorporation of the zeolite and Terfenol-D particles.

Comparing the four different drug release systems prepared (loaded zeolites; loaded membranes; membranes with loaded zeolites; and membranes with loaded zeolites and Terfenol-D under magnetic fields) it is clear that the systems present significant differences in the release kinetics and mechanisms. The membranes containing IBU-loaded zeolites appear to present a combination between the release of IBU-loaded membranes and the IBU-loaded zeolites. The release assays with the membranes containing loaded zeolite and Terfenol-D particles confirmed the influence of the applied magnetic fields in the release ratio. When the trigger is applied the Korsmeyer-Peppas model indicates a super case-II transport, indicating that the release of the drug is being driven mostly by a swelling or erosion mechanism, explained by the movement of the magnetostrictive particles when subject to the magnetic field.

KEYWORDS: Zeolites, poly(L-lactic acid), molecular modelling, controlled release, magnetic stimuli

TABLE OF CONTENTS

ACKNOWLEDGMENTS	V
RESUMO	VII
ABSTRACT	IX
TABLE OF FIGURES	XIII
LIST OF TABLES	XV
LIST OF ABBREVIATIONS	XVI
1.1. INTRODUCTION	19
1.2. COMPOSITION AND CHEMICAL STRUCTURE	20
1.3. INCORPORATION OF GUEST COMPOUNDS	21
1.4. ZEOLITES AS CONTROLLED RELEASE VEHICLES	22
1.4.1. IMPORTANCE OF THE SI/AL RATIO	22
1.4.2. STRUCTURE AND PORE SIZE INFLUENCE	23
1.4.3. EXTERNAL PH AND IONIC STRENGTH INFLUENCE.....	24
1.5. INTEGRATION OF ZEOLITES IN A TRIGGERED DRUG DELIVERY PLATFORM	30
1.6. HYPOTHESIS	31
CHAPTER 2: MATERIALS AND METHODS	33
2.1. SELECTION OF A SUITABLE ZEOLITE	35
2.1.1. MOLECULAR MODELLING OF DRUG-HOST INTERACTIONS	35
2.1.2. EXPERIMENTAL VALIDATION '	37
2.2. POLY(L-LACTIC ACID) MEMBRANES PREPARATION	39
2.2.1. POLYMER CONCENTRATION OPTIMIZATION	39
2.2.2. INCORPORATION OF IBUPROFEN.....	39
2.2.3. INCORPORATION OF THE ZEOLITE	40
2.2.4. INCORPORATION OF TERFENOL-D PARTICLES AND LOADED ZEOLITES.....	40
2.3. RELEASE ASSAYS FROM THE PREPARED MEMBRANES	41
2.3.1. EXPERIMENTAL DESIGN	41
2.3.2. RELEASE ASSAYS UNDER MAGNETIC FIELD	41
2.3.3. DRUG RELEASE MATHEMATICAL MODELS	42
2.4. CHARACTERIZATION TECHNIQUES	43
2.4.1. SCANNING ELECTRON MICROSCOPY.....	43
2.4.2. DIFFERENTIAL SCANNING CALORIMETRY	43
2.4.3. THERMO-GRAVIMETRIC ANALYSIS.....	44
2.4.4. FOURIER-TRANSFORMED INFRARED SPECTROSCOPY.....	44

CHAPTER 3: EXPERIMENTAL SECTION	45
3.1. THEORETICAL MODELLING OF IBU ENCAPSULATION.....	47
3.2. EXPERIMENTAL STUDIES OF IBUPROFEN ENCAPSULATION	50
3.2.1. FTIR STUDIES	51
3.2.2. THERMO-GRAVIMETRIC ANALYSIS.....	51
3.2.3. DRUG RELEASE PROFILES.....	52
3.3. POLY(L-LACTIC ACID) MEMBRANES PREPARATION	56
3.3.1. POLYMER CONCENTRATION OPTIMIZATION	56
3.3.2. RELEASE OF IBUPROFEN FROM THE PREPARED MEMBRANES.....	58
3.4. INCORPORATION OF THE ZEOLITE IN THE POLYMERIC MEMBRANES.....	59
3.5. PROOF OF CONCEPT – MAGNETICALLY MODULATED DRUG RELEASE	61
3.6. COMPARISON OF THE PREPARED DRUG RELEASE SYSTEMS	613
CONCLUSIONS AND FUTURE PERSPECTIVES	65
REFERENCES.....	71

TABLE OF FIGURES

Figure 1.1: Zeolite structures. Silicon atoms are placed at the vertices.....	20
Figure 1.2: Zeolitic pore unidimensional (A), bidimensional (B) and tridimensional (C) frameworks.....	20
Figure 1.3: Ibuprofen (IBU) delivery from tested zeolites and from MCM-41 (2.5nm pore), included as reference.. ..	23
Figure 1.4: Paraquat release from unmodified (black markers) and modified (white markers) zeolites for 14 days in the presence of different ion concentrations	24
Figure 1.5: pH-dependent ketoprofen release from zeolite X.	25
Figure 2.1: Schematic representation of the four key contributions to a molecular mechanics force field.	36
Figure 2.2: Disassembled (left) and assembled (right) modified glass vial used in drug release assays, with a submerged membrane (red rectangle).	41
Figure 3.1: Zeolitic structures used in the theoretical modelling studies.	47
Figure 3.2: Mean Square Displacement of the Ibuprofen molecule in each zeolitic structure.....	49
Figure 3.3: Structures of the studied zeolites.....	49
Figure 3.4: FTIR spectra of the zeolite, the drug and drug loaded carrier.....	51
Figure 3.5: Thermo-gravimetric analysis of nano-FAU zeolites loaded with ibuprofen using different solvents...51	
Figure 3.6: Ibuprofen (IBU) release from nanosized Na ⁺ -form faujasite with a 5.1 Si/Al ratio. Hexane (C ₆), ethanol (EtOH) and acetone (Act) were used as loading solvents	54
Figure 3.7: Ibuprofen (IBU) release from Na ⁺ -form Faujasite with a 5.1 Si/Al ratio. Hexane (C ₆), ethanol (EtOH) and acetone (Act) were used as loading solvents.....	54
Figure 3.8: Ibuprofen (IBU) release from Beta polymorph alpha (BEA) and Faujasite (FAU) with different Si/Al ratios and counter-ions. Hexane was used as loading solvent.	55
Figure 3.9: Ibuprofen (IBU) release from different zeolitic structures with different Si/Al ratios. Hexane was used as loading solvent.	56
Figure 3.10: Scanning electron micrographs of poly(L-lactic acid) (PLLA) membranes.....	57
Figure 3.11: Differential scanning calorimetry thermogram of the prepared poly(L-lactic acid) membranes.....	58
Figure 3.12: IBU release from PLLA membranes during 48 hours. Average \pm STD; n=3.	59
Figure 3.13: Scanning electron micrographs of 5 (wt./vol.)% poly(L-Lactic acid) (PLLA) membranes embedded with the nanosized FAU zeolites.....	60
Figure 3.14: Differential scanning calorimetry thermogram of simple PLLA membranes and PLLA membranes containing zeolite (PLLA:FAU ratio of 2:1)	61
Figure 3.15: IBU release from PLLA membranes containing IBU-loaded FAU and Terfenol-D. One sample was subject to an AC field (0 to 0.2T) during the first 8hours of the experiment. Average \pm STD; n=2.	61

LIST OF TABLES

Table 1.1 – Studies using zeolites as drug delivery systems.	26
Table 2.1 – Drug release mathematical models.	42
Table 2.2 – Exponent n of the Korsmeyer-Peppas model and drug release mechanism from cylindrical polymeric drug release systems.	43
Table 3.1 – Zeolites tested during the optimization stage.	50
Table 3.2 – Drug loading of all tested samples of zeolites.	53
Table 3.3 – Release kinetics results from the tested ibuprofen-loaded membranes.	59
Table 3.4 – Release kinetics results from the tested membranes containing IBU-loaded FAU and Terfenol-D... ..	62
Table 3.5 – Release kinetics results from the prepared drug release systems.	624

LIST OF ABBREVIATIONS

5-FU	5 - Fluorouracil
Act	Acetone
AMX	Amoxicillin
ASA-	Acetylsalicylic acid
BEA	Beta polymorph-A
BSE	Backscattered electrons
CEX	Cephalexin
CHCA	α -cyano-4-hydroxycinnamic acid
Diox	1,4 – Dioxane
DRS	Drug release system
DSC	Differential scanning calorimetry
EtOH	Ethanol
FAU	Faujasite
FER	Ferrierite
FTIR	Fourier-transformed Infrared spectroscopy
HCT-15	Human colon carcinoma cell line
HEU	Heulandite
IBU	Ibuprofen
KET	Ketoprofen
LTA	Linde-type A
LTT	Linde-type T
MCF7	Human breast adenocarcinoma cell line
MFI	Socony Mobil Five
MIT	Mitoxantrone
MOR	Mordenite
MRSA	Methicillin-resistant <i>Staphylococcus aureus</i>
MSD	Mean square displacement
MSSA	Methicillin-sensitive <i>Staphylococcus aureus</i>
Nano FAU	Nanosized (~250nm) faujasite
NO	Nitric oxide
PAAc	Poly(acrylic acid)
PAAm	Poly(acrylamide)
PBS	Phosphate buffer saline
PC-3	Human prostate adenocarcinoma cell line
PEG	Polyethylene glycol
PLLA	Poly(L-lactic acid)
PTFE	Poly(tetrafluoroethylene)
RKO	Human colon carcinoma cell line
RSV	Resveratrol
SE	Secondary electrons
SEM	Scanning electron microscopy
TGA	Thermo-gravimetric analysis
UV/Vis	Ultraviolet/visible spectroscopy
Z	Atomic number
ZER	Zerumbone

CHAPTER 1:

ZEOLITES - NEW POSSIBILITIES FOR DRUG DELIVERY SYSTEMS

1.1. INTRODUCTION	19
1.2. COMPOSITION AND CHEMICAL STRUCTURE	20
1.3. INCORPORATION OF GUEST COMPOUNDS.....	21
1.4. ZEOLITES AS CONTROLLED RELEASE VEHICLES	22
1.4.1. IMPORTANCE OF THE Si/Al RATIO	22
1.4.2. STRUCTURE AND PORE SIZE INFLUENCE	23
1.4.3. EXTERNAL PH AND IONIC STRENGTH INFLUENCE.....	24
1.5. INTEGRATION OF ZEOLITES IN A TRIGGERED DRUG DELIVERY PLATFORM.....	30
1.6. HYPOTHESIS	31

1.1. INTRODUCTION

Conventional therapy is based on the administration of the therapeutic agent frequently without any protection (other than possible excipients) or targeting moiety. Even though occasionally, a prodrug form is administered to improve some characteristics such as the drug's half-life in the organism, some drugs are poorly soluble in water or have low molecular weight, leading to an accumulation in unwanted body compartments and sometimes failing to successfully reach the target [1]. All these factors are important contributions to the poor drug bioavailability and consequently, a reduced therapeutic response. Thus, conventional therapy has been revealing itself ineffective, increasing the demand for more adequate solutions.

Nanomedicine plays an important role filling the breaches in a faulty therapeutic approach by improving the drug bioavailability. This is achieved by protecting it inside a carrier (e.g. hydrogel, nanocapsule or micelle) and by using targeting moieties or exploiting physiological flaws caused by the subjacent disease (such as the enhanced permeability and retention effect in cancer) to accumulate the drug in the desired location [2]. Another important factor is the capacity of a given carrier to reach and deliver the content specifically in the affected site or cells with any, or negligible, leakage during its path, therefore reducing undesirable side-effects. This can be accomplished not only with targeting moieties, but also with stimuli responding carriers [2–4]. Current literature presents numerous studies regarding drug release systems (DRSs) in a wide variety of forms: polymeric nanoparticles and membranes, liposomes, hydrogels, lipid nanoparticles, among many others [1,5,6].

In the latest years, zeolites have also seized some attention in the area of drug delivery. These inorganic particles were traditionally used as molecular sieves in several applications to capture numerous compounds. Exploring this characteristic, several groups exploited the highly porous matrix of the zeolites to incorporate different molecules, using them as drug delivery vehicles [7–11]. Zeolites are inexpensive, are present in numerous forms and structures and present tuneable characteristics such as its hydrophobicity and its pore size. Also, reports recognize zeolites as biologically inert particles and consider them appropriate for biological applications [11–13].

1.2. COMPOSITION AND CHEMICAL STRUCTURE

Zeolites are inorganic crystalline materials composed of SiO_4^{4-} and AlO_4^{5-} groups, which are arranged in channels and cages with well-defined structures (Figure 1.1). These channels are accessible from the surrounding medium allowing the access by numerous molecules, thus providing zeolites the ability to adsorb considerable amounts of diverse compounds [14].

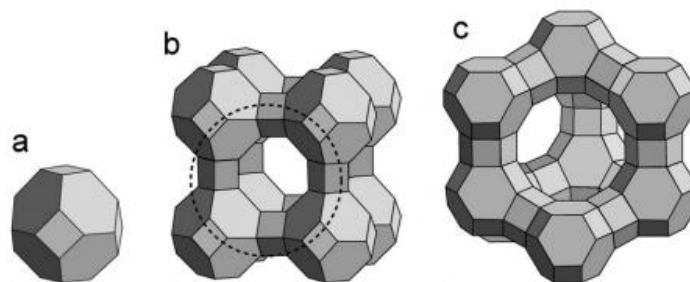


Figure 1.1: Zeolite structures. Silicon atoms are placed at the vertices.

Keys: (a) Sodalite or (β -) cage; (b) zeolite A: the β -cages are linked to each other via double four-membered rings and form an α -cage denoted by dashed circle; (c) Faujasite structure (FAU): the β -cages are connected via double six-membered rings and arranged as in the diamond lattice, forming a “super cage”. Adapted from [15]

The AlO_4^{5-} group provides an extra negative charge when replacing the SiO_4^{4-} group, thus zeolites with a decreased Si/Al ratio present higher hydrophilicity. Therefore, the degree of the zeolite hydrophobicity can be controlled by modifying the Si/Al ratio, with high Si/Al ratios ranging up to 500 and the lowest ratio being 1 [16]. The negative charge caused by the AlO_4^{5-} groups has to be neutralized with organic or inorganic cations to assure the electroneutrality of the solid. Moreover, the arrangement of the zeolite channel system is also important when incorporating molecules, with zeolites being classified in uni-, bi- or tri-directional, if the pores are organized in one, two or three axes (Figure 1.2). Due to wider pore systems, tri-directional zeolites present higher diffusion coefficients, allowing an easier incorporation but also a fast release of compounds [17].

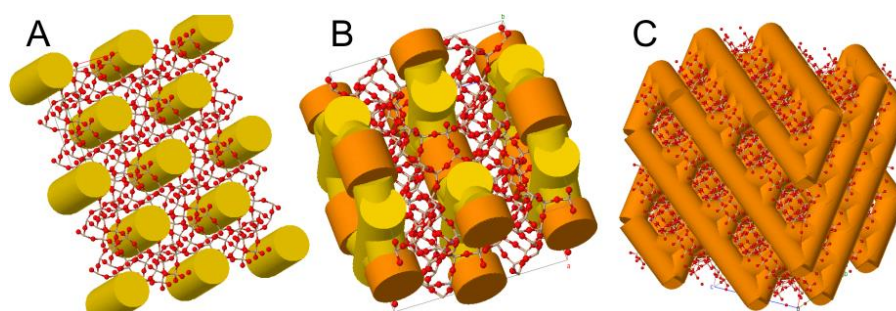


Figure 1.2: Zeolitic pore unidimensional (A), bidimensional (B) and tridimensional (C) frameworks. Only main pore frameworks are shown. Small pore systems with diameter $<4\text{\AA}$ are ignored due to negligible access by compounds of interest. From [18]. **Keys:** Yellow pores - diameter $4\text{-}6\text{\AA}$; Orange pores - diameter $>6\text{\AA}$.

Additionally to pore organization, pore size and volume are also important to modulate the entrapment or release of compounds and can be controlled during zeolite synthesis or with post-synthetic reactions [8].

Currently, a zeolite database exists with over 200 entries, where zeolites are denoted as a 3-letter code [19]. This database presents a wide number of zeolites with their structure fully characterized [18], accessible as an online database of structures and with a web tool for a 3D automated approach freely available.

1.3. INCORPORATION OF GUEST COMPOUNDS

There are several techniques to incorporate different compounds in zeolites. The chosen technique depends on the zeolite and on the substance to incorporate. Neutral molecules can be incorporated simply by dissolving them in an inert solvent in contact with the zeolite and, with continuous stirring, diffusion-guided migration will occur. The type of solvent will influence the diffusion coefficients due to different polarities and possible interactions with the zeolite [14]. Also, in hydrophilic zeolites water must be removed before the inclusion of any other molecule by heating the zeolite above 100°C [14].

For the incorporation of cationic guests to take place an ion exchange with the stabilizing cation is needed. The success and the efficiency of the exchange depends on the compound to incorporate and also on the stabilizing cation. Usually the incorporation is carried in water and often repeated with increasing concentrations of the molecule to incorporate to assure high exchange ratios [20].

Guests can also be incorporated in the gas phase using chemical vapour deposition chambers. This method is only possible at low reactional pressures or by heating the compound to incorporate at adequate temperatures (if possible). When conceivable, this method facilitates the inclusion of the desired molecule due to the absence of solvents and also prevents solvent contamination in the final product [14,21,22].

In some cases, for example when faujasite (FAU) is used, guest molecules are small enough to fit in the “super cage” (with ~1.3nm in diameter) but oversized to pass through the pore network (with ~0.7nm). When this occurs, it is possible to add a precursor into the zeolite that will eventually be transformed in the final guest. This method is usually termed “ship-in-a-bottle synthesis” [14]. Once synthesized, the guest can no longer exit the zeolite, remaining entrapped without any covalent linkage. Several cases are reported in the literature using this method, for example to immobilize fluorescent dyes for

cellular imaging [23] or to be used as catalysts in hydroxylation processes [24,25] and electro [26] or photo catalysis [27].

1.4. ZEOLITES AS CONTROLLED RELEASE VEHICLES

Zeolites were already reported as possible vehicles for controlled release of fertilizers [28], pesticides [20], preservatives [7] and, more recently, several therapeutic agents such as anti-inflammatory [6,8,22,29], antibiotics [10,30] or anticancer drugs [9,31,32]. Moreover, studies have shown the biological inertia of these compounds [12,13], allowing their use in biological applications. Thus, their unique characteristics (rigid structure, high adsorption ratios, tuneable hydrophobicity, controlled pore size and biological inertia) allow zeolites to be a promising alternative as carriers in controlled release DRS, providing an increase of the drug loadings and also delaying the initial release of the drug creating a sustained and prolonged release [33].

There are, however, some parameters to revise when using zeolites as drug carriers. The type of drug-host interaction is of great importance. If, for example, the interaction is based on ion exchanges, the external pH and the Si/Al ratio will greatly influence the release rate. Also, the drug to incorporate must be properly chosen because, due to the zeolites' well-defined and rigid structure (with restricted pore and cage diameters), the possible drugs to encapsulate are size-limited. Surface modifications are sometimes useful to slow the release by decreasing pore size, delaying the diffusion rate from minutes to days. Some examples illustrate the effect of distinct zeolite characteristics and their importance for the selection of both zeolite and drug to yield a functional and balanced DRS.

1.4.1. IMPORTANCE OF THE Si/Al RATIO

Horcajada and colleagues studied the influence of the Si/Al ratio on the release of ibuprofen (IBU) from FAU [8]. In this study, four zeolites were used: Z100, Z712, Z720 and Z760, with Si/Al ratios of 7, 13, 22 and 62, respectively. The Z100 zeolite showed the lowest IBU internalization (72mg IBU/g) with 4 IBU molecules per unit cell, while the other tested zeolites presented IBU internalization of 150-160mg/g (approx. 9 IBU molecules per unit cell). These results suggest that there is a maximum amount of drug capable of fitting in the zeolite structure. The drug release assay (Figure 1.3) showed a slower IBU release from Z100 and Z712 comparing to Z720 and Z760. FTIR analysis revealed that in Z100 and Z712 the interaction with IBU occurs due to coordination with the extra-framework aluminium, while in

Z720 and Z760 this interaction occurs *via* hydrogen bonding (weaker bond), explaining the difference in the drug release rates.

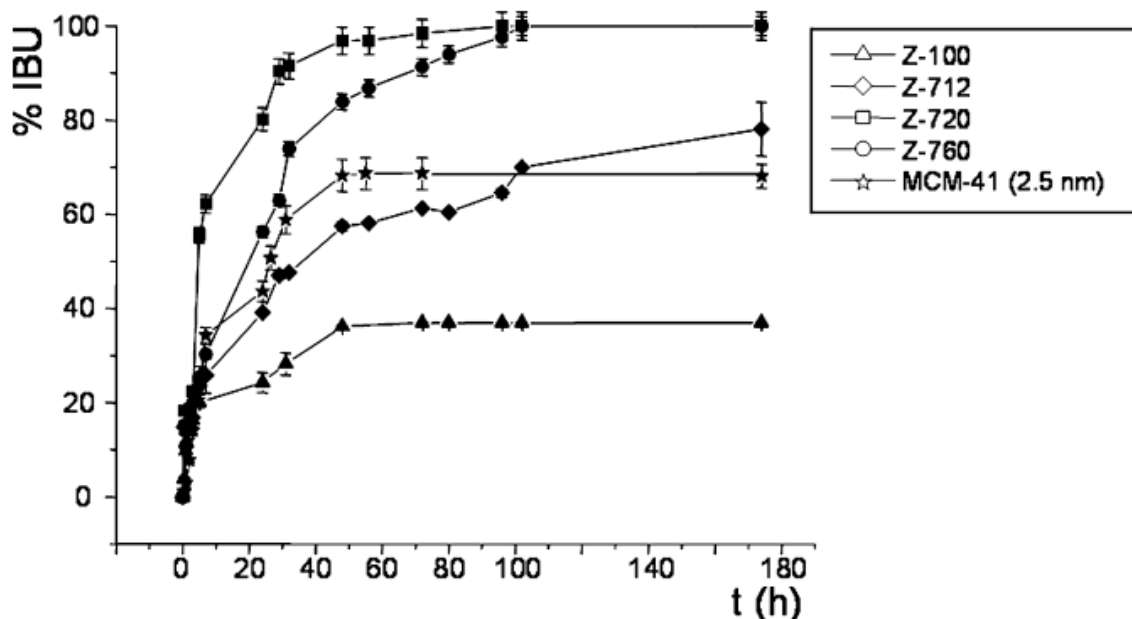


Figure 1.3: Ibuprofen (IBU) delivery from tested zeolites and from MCM-41 (2.5nm pore), included as reference. Zeolites Z100, Z712, Z720 and Z760, with Si/Al ratios of 7, 13, 22 and 62, respectively. From [8].

1.4.2. STRUCTURE AND PORE SIZE INFLUENCE

Showing the importance of structure and pore size of the zeolites, Fisher and co-workers studied the uptake of different species of fluorescein (fluorescein sodium salt, fluorescein free acid, and fluorescein diacetate) by Zeolite X (FAU framework with a low Si/Al ratio) and MCM-41 (a mesoporous silicate material with pores with 2 - 6.5nm) [34]. The results indicated that there was little uptake of this compounds within the zeolite pores, possibly due to the excessive size and rigidity of the fluorescein molecule, resulting only in surface adsorption of small amounts. Contrarily to expected, the increased pore size of MCM-14 did not cause a substantial increase in the uptake of all species of fluorescein. Other studies have already reported that materials with larger pores do not always result in higher uptakes [35] due to the influence of the loading solvent and the hydrophobicity of the loaded molecule and the carrier structure itself.

In a different study, pore size of Zeolite Y was modified by Zhang *et al.* using 1,1,3,3-tetramethyldisilazane [20] to assess its influence on the release of paraquat, a herbicidal drug. After the incorporation of the drug, the zeolites were dehydrated and modified with the silanol groups. Without the modification, the authors observed that the release of paraquat reached a plateau after 20min. However, with the

coupling of the silanol groups, the release occurred at different rates, with a plateau being observed only after 7 days of release (Figure 1.3). Hence, pore engineering is an efficient pathway to control the drug release from zeolites, with different possible release rates depending on the modifying agent used.

1.4.3. EXTERNAL PH AND IONIC STRENGTH INFLUENCE

In the same study, Zhang and co-workers also verified the importance of the ionic strength of the release medium [20]. When $[\text{NaCl}] = 1\text{M}$, all paraquat was released from the interior of the tested zeolites, however, when the salt concentration decreased to 0.1M and 0.01M, only 65% and 14% of the loaded paraquat was released, respectively (Figure 1.4).

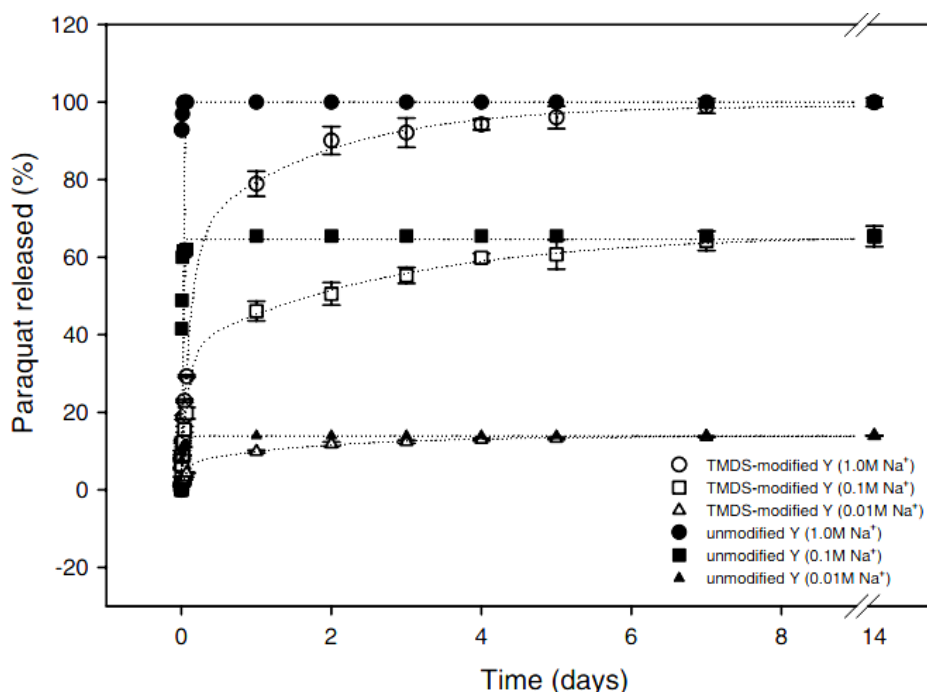


Figure 1.4: Paraquat release from unmodified (black markers) and modified (white markers) zeolites for 14 days in the presence of different ion concentrations (circles: 1.0M Na⁺; squares: 0.1M Na⁺; triangles: 0.01M Na⁺). From [20].

Taking into account that zeolites possess negative charges, which are stabilized by counter-ions, Payne and Abdel-Fattah studied the effects of pH and ionic strength on the adsorption of Pb²⁺ ions onto Zeolite A and Zeolite X (both with Na⁺ as counter-ion) [36]. The study was conducted by simply adding the zeolites to an aqueous lead solution (at different pH's and with different amounts of KNO₃) at room temperature with aliquots being collected at different time periods. A more extensive ion-exchange was observed when the pH reached 4 and above. Also, the presence of competing ions in the medium revealed to significantly decrease the lead adsorption.

Furthermore, Rimoli and colleagues studied the release of ketoprofen (KET), an anti-inflammatory drug, from Zeolite X at different pH values, mimicking the pH changes in the digestive tube [6]. The authors found that at highly acidic pH, there was only a residual release of the drug, while at pH5 a progressive release started which was accelerated when the pH increased to 6.5 (Figure 1.5). This behaviour was related to the ionization of the carboxylic group of the drug at pH 5, causing an enhanced repulsion between the drug and the zeolite (both holding negative charges) leading to KET dissociation and release. This system was suggested as a possible drug delivery system with the release occurring only after the carrier has passed through the stomach acidic pH, contributing to the reduction of the adverse effects caused by oral ingestion of anti-inflammatory drugs.

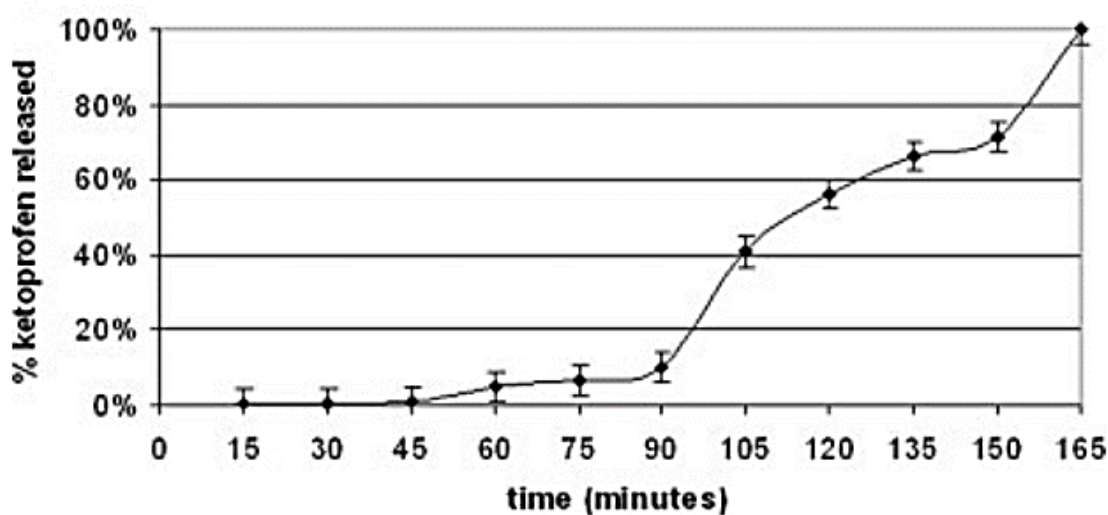


Figure 1.5: pH-dependent ketoprofen release from zeolite X. From [6].

Keys: 0-90min: pH1; 90-135min: pH5, 135-165min: pH6.8.

Hence, when considering zeolites for drug delivery several parameters ought to be considered: Drug size and hydrophobicity, loading methodology and solvent, zeolite structure, pore size, hydrophobicity and Si/Al ratio, drug-zeolite interaction and ionic strength and pH of the medium. Table 1.1 summarizes important studies involving zeolites as DRS, with some particular references to the above-mentioned characteristics. Despite the existence of several studies, occasionally comparing different frameworks or Si/Al ratios, exhaustive studies showing how the loading of a model drug is influenced by particular characteristics are scarce. Being able to understand to what extent the Si/Al ratio, the counter-ion and the zeolitic structure influence the loading of a drug is an important step to the design of a tuneable drug release platform.

Table 1.1 –Studies using zeolites as drug delivery systems.**1. COMPARATIVE STUDIES**

Substance	Zeolite framework	Si/Al ratio	Loading	Results	Observations	Refs.
IBU	FAU	7	72mg/g	IBU adsorption studies revealed an occupation of 4 IBU molecules per unit cell for FAU-7 and 8-9 IBU molecules for FAU-13, -22 and -62. All the samples possess a micropore volume close to 0.30 cm ³ /g, except FAU-7 (0.20 cm ³ /g). FAU-7 presents a negligible mesopore volume, while the other samples present volumes of 0.15-0.17 cm ³ /g. FAU 7 and -13 showed an incomplete release of IBU in the 174h study, with a drug retention of 63% and 22%, respectively. FAU-22 fully released the drug in 96h and FAU-62 in 102h.	FAU-7 high extra-framework aluminium justifies both its low pore volume (partial pore blockage) and its decreased loading capacity. The similar IBU adsorption capacity of FAU-13, -22 and -62 indicates that there is a maximum amount of drug loadable into the structure. The total pore volume of FAU-7 is nearly 50% of the remaining samples, similarly to its loading capacity. Thus, a ratio of 1.5-1.7mmol IBU/cm ³ for all samples was obtained. In samples with lower Si/Al ratios the drug is covalently bound to the structure, delaying its diffusion, while in samples with lower Al content, the retention occurs due to weaker interactions (H-bonds and van der Waals).	[8]
		13	162mg/g			
		22	152mg/g			
		62	148mg/g			
5-FU	FAU	<1.5	161.8mg/g	Release of 5-FU from FAU and BEA was significantly different. Full release occurred at 10min (FAU) and at 120min (BEA). Also, the release profiles are markedly different with FAU showing a 80% burst release in the first 3min while BEA shows a multi-step release with 15% released in the first 10min, up to 50% in the next 40min and the remaining drug within an hour. Unloaded FAU presents noticeable cell growth alterations at 8h (concentration dependent) while unloaded BEA showed no toxicity. Loaded particles showed high toxicity, similarly to the free drug.	Larger pores and pore organization are the main reasons for the difference on the loading and also release profiles, with FAU presenting larger pore diameter. The tighter pores in BEA originate much stronger short-ranged van der Waals' interactions between the drug and the zeolite, dampening the release. The difference in the toxicity of unloaded particles may be explained by their morphology, with multi-faceted FAU being able to penetrate cell membranes more easily than spherical BEA particles.	[37]
	BEA	250	60.2mg/g			

Keys: BEA – Beta Polymorph A; FAU – Faujasite; IBU – Ibuprofen; 5-FU – 5-fluorouracil.

(Table 1.1 continued)

Substance	Zeolite framework	Si/Al ratio	Loading	Results	Observations	Refs.
5-FU	FAU	5	110 mg/g	FAU-5 presented a negligible release (<5%) over a period of 6h, whereas the other 2 samples presented a release of around 60%.	5-FU forms strongly bonded complexes with the extra-framework aluminium sites, extensively hampering the release of the drug.	[38]
		30	105 mg/g			
		60	90 mg/g			
	FAU	2.83	7.2mmol/g (936mg/g)	FAU presented a higher encapsulation efficiency (71.3%) than the other samples (~50%). The release profiles revealed an 80%, 94% and 89% maximum release in 48h for FAU, nano-sized FAU and LTL respectively. A burst release occurred in the first 10minutes with 80-90% of 5-FU being released. No toxicity was found to be caused by all the samples in HCT-15 and RKO cell lines. The system showed to potentiate in 1.6-7.6 times the drug effect.	Owning a larger micropore volume, FAU presents a higher 5-FU loading capacity. The rapid release is explained by the drug's small size facilitating the diffusion from the micropores. The potentiation is explained by the increased bioavailability of 5-FU and the facilitated cell uptake. The extremely high drug loadings indicate that significant amounts of drug may be adsorbed onto the zeolite surface and not inside the pores.	[39]
	FAU (nano-sized)	2.25	5.5mmol/g (715mg/g)			
	LTL	3.4	5.2mmol/g (676mg/g)			
CHCA	FAU	2.83	78.9mg/g	No decrease in metabolic activity of HCT-15 cells caused by FAU or LTA (24h). Increase in efficiency of the drug up to 585-fold (FAU) and 146-fold (LTA) when compared to the non-encapsulated drug.	The wider structure of FAU allowed a better diffusion of the drug out of the zeolite pores, justifying the difference in the results.	[9,31]
	LTA	1.24	69.7mg/g			
ASA	FAU	5	106mg/g	Lower Si/Al ratio zeolite showed a complete release of the drug in 5hours, whereas the other two samples released only 63% of the drug in the same time. Aluminium-acetylsalicylate formed at the FAU-5 extra-framework aluminium sites due to the deprotonation at pH 7.4. With FAU-30 and -60 the deprotonation did not occur drug was bound to silanol sites via H-bonds.	As hydrophobicity increases with higher Si/Al ratios, van der Waals interactions become a contributing factor to the release profile, hindering the drug release. Aluminium-acetylsalicylate species are more weakly bound to the zeolite than the protonated form of the drug, creating the conditions for a complete release of the drug.	[40]
		30	78mg/g			
		60	69mg/g			

Keys: ASA - Acetylsalicylic acid; CHCA – α -cyano-4-hydroxycinnamic acid; FAU – Faujasite; HCT-15 – human colon carcinoma cell line; LTA – Linde Type A; LTT – Linde Type T; n.g. – not given; RKO – human colon carcinoma cell line; 5-FU – 5-fluorouracil.

(Table 1.1 continued)

2. ISOLATED STUDIES

Substance	Zeolite type	Si/Al ratio	Loading	Results	Observations	Refs.
MIT	BEA	n.g.	3.02mg/g	MIT structure does not allow a full incorporations onto the zeolitic pore system, however there is a direct interaction with the extra-framework aluminium. The 72h release studies revealed that no drug was released from the zeolite. After incubation of the system with MCF-7 and PC-3 cell lines, lower toxicity was observed when comparing to mitoxantrone alone. In the presence of the system morphological changes were observable in both cell types.	The authors hypothesize that, after ruling out the possible toxicity of the zeolite, the drug was only released once inside the cell. The delayed release justifies the decreased toxicity of the loaded zeolite comparing to the drug alone. The nanoparticles retained the optical characteristics of the mitoxantrone, yielding a useful hybrid bearing both therapeutic and cell-marking properties.	[41]
CEX	HEU	n.a.	10.5mg/g	Hexadecyl-trimethylammonium surfactant increased the adsorption of CEX on HEU. Un-buffered and phosphate buffered release mediums presented inverse release profiles with increasing pH values. At pH 2 (un-buffered) a maximum desorption was obtained, suitable for drug releasing platforms to work at gastric pH.	With a surfactant-modified zeolite the ion exchanging process between the drug and the carrier is favoured, thus increasing the loading capacity. The adsorption and desorption are affected by the presence of different ions, hence the distinct behaviour in the presence of buffered (tri-, di- and monovalent phosphate species) and un-buffered (Cl ⁻ ions) solutions.	[42]
RSV	BEA	n.g.	484 mg/g	The release profiles showed that a total release was achieved in about 3h, contrarily to free resveratrol. The encapsulation on the zeolite prevented the transformation of resveratrol from <i>trans</i> to <i>cis</i> (less active form).	The system showed an increased resveratrol solubility compares to the free drug. Also, due to the rigidity of the zeolitic pores, the isomeric conversion was impaired, preserving the bioactive form of the molecule.	[43]

Keys: BEA – Beta Polymorph A; CEX – Cephalaxin; HEU – Heulandite; MIT – Mitoxantrone; MCF-7 – human breast adenocarcinoma cell line; n.a. – not applicable; n.g. – not given; PC-3 – human prostate adenocarcinoma cell line; RSV – Resveratrol.

(Table 1.1 continued)

3. COOPERATION WITH DIFFERENT MATERIALS

Substance	Zeolite type	Si/Al ratio	Loading	Results	Observations	Refs.
ZER + Gelatine	FAU	>5	n.g.	After incorporating ZER in the zeolite, a gelatine coating layer was successfully added to the system, proving to delay the release of the drug. The system showed a sustained release for 24h (100% release) compared to the 3h release from the non-coated zeolite.	The gelatine layer swelled in contact with the releasing medium and was further eroded. During this process, the diffusion of the drug was hampered.	[32]
AMX + PEG + PAAc + PAAm	LTA	n.g.	n.g.	The loaded zeolite was incorporated on a hydrogel. The release studies were conducted by at pH 7.8 and 6.8 and at different temperatures. The composite exhibited a temperature and pH dependent release, with higher temperatures and pH causing an enhanced release.	PAAc and PAAm are polymers both responsive to temperature and pH. At higher temperatures structural changes occur, increasing the release of AMX. At higher pH values, the polymer's functional groups become ionized, increasing the repulsive forces and causing the polymer to swell. This effect increases the diffusion of the drug.	[11]
4. ZEOLITE BASED DELIVERY DEVICES						
Saline solution	MFI	n.a.	n.a.	Zeolite walled micro-needles effectively penetrated through the upper layers of 8 month old domestic pig skin. The poration of the skin caused a 1000x increase in the permeability to saline solution.	The tested system demonstrated promising results as a transdermal drug delivery system. The drug can be embedded on the zeolite's surface/pores or dissolved in a solution (e.g. saline).	[44]
NO	LTA	n.g.	n.g.	Antibacterial disks with 50 w% of PTFE and of Zn ²⁺ -exchanged zeolite revealed to release micromolar concentrations of NO over approx. 1h when in aqueous medium. The composite showed a bactericidal effect when in contact with <i>P.aeruginosa</i> and a bacteriostatic effect when in contact with MSSA, MRSA and <i>C.difficile</i> .	The system showed an improved bactericidal activity when compared to NO alone. The bacteriostatic effect on the Gram positive strains may be due to Zn ²⁺ ions leaching from the zeolites.	[45]

Keys: AMX – Amoxicillin; FAU – Faujasite; LTA – Linde Type A; MFI – Zeolite Socony Mobil – 5; MRSA – Methicillin-resistant Staphylococcus aureus; MSSA – Methicillin-sensitive Staphylococcus aureus; n.a. – not applicable; n.g. – not given; NO – Nitric oxide; PTFE – Poly(tetrafluoroethylene); PAAc – Poly(acrylic acid); PAAm – Poly(Acrylamide); PEG – Polyethylene glycol ZER – Zerumbone.

1.5. INTEGRATION OF ZEOLITES IN A TRIGGERED DRUG DELIVERY PLATFORM

As mentioned previously, several zeolite-based systems for drug delivery are reported and, whereas most of the works report the use of the zeolitic material alone, there are cases of zeolites combined with different materials [45] or incorporated in a platform [11]. The incorporation of these materials in other platforms is advantageous due to the possibility of tailoring the material.

Polymers are excellent choices to build quite distinct and unique DRSs due to their wide variety (natural and synthetics), thus offering the advantage of being highly tunable in terms of size, structure and physical-chemical properties (hydrophobicity/hydrophilicity, reactive groups, etc.) and degree of degradability depending on the application. Reports have been made of polymeric DRSs that can serve as drug carriers with sustained releases up to several months or even years [46].

Other than hydrogels or nanoparticles, polymeric membranes are also good candidates to develop drug release systems. This type of system can be extremely useful to prepare drug releasing platforms to be used, for example, as skin patches [47] or even as temporary interfaces during the healing process after surgery [48]. When a system is going to be integrated in the body, its safety has to be proven and its degradability into non-toxic sub-products is essential. Poly(L-lactic acid) (PLLA) is a well-known polymer already used in drug delivery applications [48–50] and recent reports show that exposure to PLLA membranes presents no significant cytotoxicity or genotoxicity [51] making them an excellent option as to be used as DRS.

Polymer-based DRSs can become stimuli-responsive with the insertion of, for example, an ionisable group (pH sensitivity) [52], disulphide bridges (redox sensitivity) [3] or an azobenzene derivative (light sensitivity) [53] into its backbone. This type of systems can sometimes be responsive to more than one stimulus, hence improving drug release performances [54]. The most studied and important stimuli are often divided in two categories [55]: endogenous triggers (pH, redox, glucose, enzymes, etc.) and exogenous (temperature, light, magnetic field, ultrasounds, etc.).

Polymeric structures are affected by magnetic fields when magnetic nanoparticles are incorporated onto the matrix. Several studies have reported the incorporation of magnetic particles in polymeric systems, such as hydrogels [56,57] or polymeric nanoparticles [58,59]. These systems can be used as cancer therapy agents [60], artificial muscles [61], magnetic separation [62], drug delivery systems [59], among others [3]. Magnetostriction is, by definition, the variation of the strain of a material as a quadratic function of an applied magnetic field [63,64], i.e. when in presence of a magnetic field, the material will

alter its dimensions, with Terfenol-D and CoFe_2O_4 as good examples of extensively described magnetostrictive particles [63]. The application of polymeric systems bearing magnetostrictive particles are therefore useful in drug delivery, adding an additional feature that acts as a trigger for the release of the drug.

1.6. HYPOTHESIS

Even though a variety of studies have reported the use of different zeolites as drug release platforms, the integration of drug loaded zeolites onto polymeric membranes was not yet fully accomplished. This combination can improve the DRS's features as the inclusion of a drug in a carrier that, in its turn, is going to be incorporated in a platform allows a more controlled and prolonged release. This prolonged release occurs because the drug has first to travel first through the zeolitic pores and only then exit the membrane. Also, a wider variety of guests can be incorporated in a zeolite due to the diversity of existing zeolitic structures and their tunable characteristic e.g. the hydrophobicity of a zeolite can be controlled by changing its Si/Al ratio and the counter-ion can be changed in order to allow a better ion exchange with the guest. The addition of magnetostrictive particles to the system would allow the triggered release of the guest from the platform, or at least would allow to greatly increase its release ratio.

The combination of zeolites and magnetostrictive particles in a polymer based platform presents itself as a novelty for the active release of desired drugs, hence a hypothesis was developed: the design of a polymeric drug delivery platform containing a zeolite as the drug carrier and Terfenol-D as the magnetostrictive element.

The specific objectives of this thesis are:

1. Theoretical and experimental studies the encapsulation of a model drug (IBU) onto zeolites;
2. Preparation of IBU-loaded PLLA membranes;
3. Incorporation of the zeolite in PLLA membranes;
4. Incorporation of loaded zeolite and Terfenol-D particles onto PLLA membranes and prove the magnetically-driven release of IBU.

CHAPTER 2:

MATERIALS AND METHODS

2.1. SELECTION OF A SUITABLE ZEOLITE.....	35
2.1.1. MOLECULAR MODELLING OF DRUG-HOST INTERACTIONS	35
2.1.2. EXPERIMENTAL VALIDATION '	37
2.2. PLLA MEMBRANES PREPARATION.....	39
2.2.1. POLYMER CONCENTRATION OPTIMIZATION	39
2.2.2. INCORPORATION OF IBUPROFEN.....	39
2.2.3. INCORPORATION OF THE ZEOLITE	40
2.2.4. INCORPORATION OF TERFENOL-D PARTICLES AND LOADED ZEOLITES.....	40
2.3. RELEASE ASSAYS FROM THE PLLA MEMBRANES.....	41
2.3.1. EXPERIMENTAL DESIGN	41
2.3.2. RELEASE ASSAYS UNDER MAGNETIC FIELD	41
2.3.3. DRUG RELEASE MATHEMATICAL MODELS	42
2.4. CHARACTERIZATION TECHNIQUES.....	43
2.4.1. SCANNING ELECTRON MICROSCOPY.....	43
2.4.2. DIFFERENTIAL SCANNING CALORIMETRY	43
2.4.3. THERMO-GRAVIMETRIC ANALYSIS.....	44
2.4.4. FOURIER-TRANSFORMED INFRARED SPECTROSCOPY.....	44

2.1. SELECTION OF A SUITABLE ZEOLITE

More than two hundred zeolitic structures are already described, each with particular characteristics suitable for different goals. As already presented in Table 1.1, only a few structures are usually selected when using zeolites as drug carriers. In order to being able to properly adequate the choice of the zeolite to the desired loading and release parameters, a screening of different structures with different counter-ions and Si/Al ratio was conducted.

In a first phase, molecular simulations were conducted with five different frameworks: FAU, BEA, MFI, Mordenite (MOR) and Ferrierite (FER). The aim was to study the influence of the zeolitic structure on the drug diffusion through the pores and channels, possibly allowing to understand how the structure could influence the loading and the release of the drug.

In a second stage, experimental tests were performed with the structures selected by the molecular modelling. This would allow to confirm the results of the simulations, but also to test further variables, such as the influence of the loading solvent, counter-ions and Si/Al ratio.

2.1.1. MOLECULAR MODELLING OF DRUG-HOST INTERACTIONS

When incorporating molecules inside well characterized and rigid zeolitic pore systems it is of great importance to understand not only how much of that compound can be fitted in the zeolite but also how will the drug interact with the host. Using a molecular modelling software, some interactions and behaviours can be studied. The modelling can be achieved by two computational mechanics: quantum mechanics and molecular mechanics.

Quantum mechanics explicitly models the electrons of each atom, being possible to derive proprieties that depend upon the electronic distribution, particularly when investigation chemical reactions or formations and cleavage of bonds. The starting point of all quantum mechanics calculations is, therefore, the Schrödinger equation. This consideration is the principal differentiation between quantum mechanics and the empirical force fields used in molecular mechanics – the modelling of individual electrons [65].

Molecular mechanics, on the other hand, ignores the electronic contribution and calculates the energy of a system based on the nuclear positions only, using empirical force fields. This is particularly useful when dealing with systems with a significant number of atoms, since when ignoring the electrons, a substantially smaller number of particles are considered, thus largely reducing the computation time. The

majority of the force fields used for molecular systems can be depicted using a simple four-component representation of the intra and intermolecular forces (Figure 2.1).

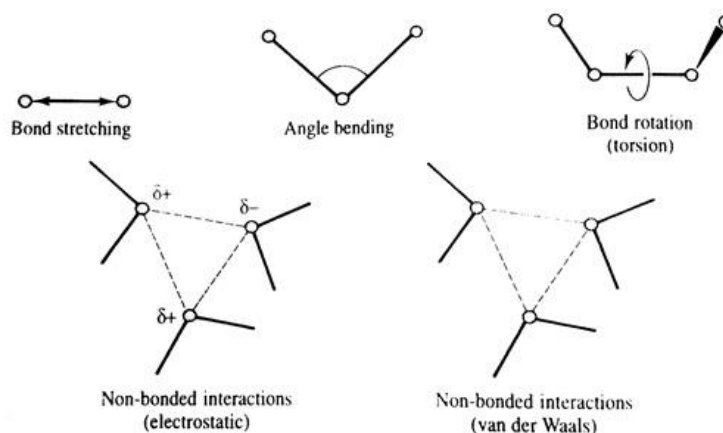


Figure 2.1: Schematic representation of the four key contributions to a molecular mechanics force field. From [65]

The total energy of the system can then be calculated summing the contributions of bond stretching, angle bending, bond torsion and non-bonded interactions (electrostatic and van der Waals interactions) [65] as depicted in:

$$E_{tot} = \sum E_{bond} + \sum E_{ang} + \sum E_{torsion} + \sum E_{non-bond} \quad (\text{Equation 2.1})$$

Where $\sum E_{bond}$ represents the bond stretching energies, $\sum E_{ang}$ represents the angle bending energies, $\sum E_{torsion}$ represents the energy of torsional movement (bond rotation) and $\sum E_{non-bond}$ represents non-bonded interactions (electrostatic and van der Waals).

The calculation the energy of a system is not, however, enough to model the movement of molecules in contact with a solvent or imprisoned in a carrier. To do so, molecular dynamics simulations are needed. In these simulations, successive configurations of the system are generated by the applications of Newton's laws of movement, generating a trajectory that determines how the position and velocities of the particles in the system vary with time. The trajectory is obtained by solving the differential equations resulting from Newton's second law [65]:

$$\frac{d^2x_i}{dt^2} = \frac{F_{x_i}}{m_i} \quad (\text{Equation 2.2})$$

Where m_i is motion of a particle of mass along a coordinate (x_i), with F_{x_i} being the force on the particle in that direction at time t .

Throughout the literature it is possible to find studies in which theoretical and experimental results are performed in parallel [15,16,37,66], allowing to better understand some of the experimentally obtained data, or even to eliminate some possibilities prior to the experimental studies.

The molecular dynamics simulations can show how a specific drug molecule will move inside the zeolitic framework over time and, in the specific case of zeolite based drug delivery systems, this can be used to explain different loading efficiencies or different drug release rates obtained when using different zeolitic structures or different drugs [37].

Materials Studio molecular modelling software was used to model distinct drug-host interactions. The study was conducted by placing a drug molecule inside each zeolitic structure, followed by a geometry optimization in order to reduce the energy (and consequently, the interactions). The drug-host complex was then subject to a molecular dynamic simulation, at 310K, using the Forcite module with a universal force field.

2.1.2. EXPERIMENTAL VALIDATION

After the molecular modelling simulations, an experimental phase was planned. In this stage, the previously selected structures were used, bearing different counter-ions (Na^+ , NH_4^+ and H^+) and also different Si/Al ratios.

2.1.2.1. LOADING TECHNIQUE

The chosen loading technique consisted in placing the zeolite in an IBU solution for 24h as described [37,38]. Aiming the optimization of the process, this method was conducted using three different solvents. Ethanol (EtOH, 95% v/v, extra pure, Fisher Scientific), Acetone (Act, Laboratory Reagent, $\geq 99.5\%$, Sigma-Aldrich) and n-Hexane (Hex, analytical reagent grade, Fisher Scientific) were chosen due to their different polarities and functional groups and also because they were already reported as loading solvents [8,37,39]. Before the utilization of the zeolite, a dehydration step was performed by placing the zeolite at 100-110°C overnight. This step is important to remove the water trapped in the pores of the zeolite, which otherwise would severely decrease the drug loading [14]. Briefly, 500mg of the zeolite and 250mg of IBU were placed in a glass vial and 10mL of the selected solvent was added, always ensuring that completely solubility of IBU. The mixture was kept under stirring for 24h. Next, a filtration process was conducted, with a Whatman® Ashless, grade 40 filter paper. After the procedure, the zeolite was retrieved and kept

at 50°-60°C for 4-6h for the complete removal of the remaining solvent. The final product was labelled IBU@(zeolite structure) e.g. IBU@FAU (ibuprofen at faujasite).

2.1.2.2. RELEASE ASSAY

In order to evaluate both the loading and the release kinetics, release assays were conducted using a USP-1 dissolution apparatus (Erkwa instruments; basket; 50rpm). In this apparatus, the zeolite was placed in 1000mL of Phosphate buffer saline (PBS) pH 7.4 at 37°C. Aliquots were taken at specific time-points by a flow system, using a peristaltic pump, which was connected to a UV/Vis-spectrophotometer (Thermo Spectronic UV-500) and the released IBU was quantified. After the readings, the collected sample returned to the release medium, keeping a constant volume throughout the experiment.

IBU Quantification by UV/Vis-spectroscopy (UV/Vis)

UV/Vis is a widely used technique to quantify different analytes. This method is based on Beer-Lambert law which relates the light transmitted through a solution with, among other parameters, the concentration of an existing substance [67]:

$$A = \alpha \times l \times c \quad (\text{Equation 2.3})$$

Where A is the absorbance, α is the molar extinction coefficient, l is the optical path length and c is the concentration of a present substance.

The first step was the acquisition of a calibration curve within a linear range of concentrations and with values that would fit the concentrations used during the work. Initially a stock solution of 600mg/L of ibuprofen in PBS was prepared which was then properly diluted in order to obtain the desired standard samples used in the calibration curve. The measurements were performed using the same spectrophotometer described in the above section, reading the absorbance at a wavelength of 264nm. A linear regression was applied to the obtained calibration curve and presented an $R^2=0.9946$ and the equation $Y = 0.002X+0.0027$.

PBS solution preparation

For the release kinetic assays, a 10xPBS 0.1M stock solution was prepared. The following quantities were used to prepare 1000mL of 10xPBS: 9.94g (70mM) of Disodium hydrogen phosphate (Na_2HPO_4 anhydrous, ChemAlert); 4.14g (30mM) of Sodium dihydrogen phosphate ($\text{KH}_2\text{PO}_4 \cdot \text{H}_2\text{O}$, ChemAlert) and 75.97g (1.3M) of Sodium chloride (NaCl, analytical reagent grade, Fisher Scientific).

Prior to use, the 10xPBS solution was diluted 10 times with deionized water and the final PBS had a pH 7.4 and a final concentration of 10 mM phosphate and 130 mM NaCl.

2.1.2.3. DETERMINATION OF IBU LOADING ONTO ZEOLITE

After the quantification of the drug, its loading amount (% wt.) was calculated using equation 2.4:

$$\text{Loading (\% wt.)} = \frac{\text{Drug mass in zeolite}}{\text{Loaded zeolite mass}} \times 100 \quad (\text{Equation 2.4})$$

2.2. POLY(L-LACTIC ACID) MEMBRANES PREPARATION

Poly(L-lactic) acid (PLLA, average molecular weight of 217,000–225,000g/mol) membranes were prepared through an adapted freeze-drying method [68,69]. In this technique, the polymer is placed in a solvent, the solution is casted on a surface and then freeze dried. During this work, 1,4-dioxane (Diox, anhydrous, 99.8% grade, Sigma-Aldrich) was used as solvent for the preparation of the membranes. Due to a melting point of 11.8°C, 1,4-dioxane will rapidly freeze at the low temperatures of an ice bath (approx. 0°C) or a simple freezer (approx. -20°C). This feature is important to keep the homogeneity of the membrane when incorporating the zeolite or the magnetic nanoparticles. The prompt freezing maintains a good dispersion of the particles, which could be lost if the dispersion is kept in the liquid state for a long period. Also, the solvent plays an important part in the pore system development, acting as porogenic. As the temperature decreases and solvent freezes, the polymer will “surround” the solvent crystals, thus giving rise to a pore when the solvent is removed.

2.2.1. POLYMER CONCENTRATION OPTIMIZATION

In order to assess the suitable membranes to be used as drug carriers, several optimizations were performed. The first was the determination of the amount of polymer to be used during the preparation of the membranes. To do so, several polymer concentrations were used: 1, 3, 5 and 10 (wt/vol.)%. Briefly, the desired amount of polymer was placed on a glass vial with 2.3cm of internal diameter, 1mL of solvent was added and kept under stirring until complete dissolution. The solutions were then placed at -20°C and later freeze-dried. After the freeze-drying process, the membranes were characterized.

2.2.2. INCORPORATION OF IBUPROFEN

During the preparation of the membranes with IBU (purity ≥98%, Sigma-Aldrich), the additional step was the incorporation of the drug in the polymer solution, followed by the same procedure described in

the above section. In this phase, different quantities of IBU were added to study the effect of different loadings on the drug release profile. The obtained membranes contained a final concentration of 3, 5 and 10 wt% of IBU and were later characterized and subject to drug release assays.

2.2.3. INCORPORATION OF THE ZEOLITE

The following step was the development of PLLA membranes containing the zeolite (Freeze-dried Na⁺-form of Faujasite (Nano FAU), particles sizes averaging 150nm, NanoScape). This required the dispersion of the zeolite in the solvent in an ultrasound bath for 4h prior to the addition of the polymer. Again, different amounts of Nano FAU were added to 1,4-dioxane, now aiming to assess the influence of the solid on the membrane pore structure. The prepared membranes contained a final zeolite:PLLA mass proportion of 20, 10, 6, 4 and 2:1. Prior to all preparations, the zeolite was placed at 180°C overnight in order to remove any adsorbed water.

2.2.4. INCORPORATION OF TERFENOL-D PARTICLES AND LOADED ZEOLITES

The last step involving the development of the PLLA membranes was the incorporation of the Terfenol-D particles (from ETREMA) and drug loaded zeolite. Terfenol-D particles are not dispersible in Diox alone due to their high molecular weight. Consequently, previous to the dispersion, the polymer was added to the solvent in order to increase the viscosity of the medium. Next, the Terfenol-D particles were added and placed on an ultrasound bath for 10min. Next, drug loaded zeolite was added to the dispersion and kept under ultrasounds until complete dispersion of both magnetic and zeolitic particles. While the sample was in the ultrasound bath, the water temperature was decrease with the addition of ice. This caused the solvent to freeze, thus maintaining a good dispersion of the particles when the preparation was removed from the ultrasounds. The final product was then placed at -20°C and freeze-dried. Due to more desirable characteristics, the membranes chosen for this phase were prepared with 5 (wt/vol.%) of polymer in 1mL of solvent, and the membrane's components final concentration were 65 wt% of PLLA, 15 wt% of Terfenol-D and 20 wt% of IBU@FAU. The amount of Terfenol-D used was previously optimized in order to obtain the desired magnetostritive effect without compromising the stability of the membrane [70] . These membranes were then used to study the drug release profile in the presence and absence of magnetic fields.

2.3. RELEASE ASSAYS FROM THE PREPARED MEMBRANES

After the loading of the membranes, an evaluation of the release kinetics from membranes loaded with IBU or with IBU@FAU was conducted. The release was again conducted in PBS pH7.4 at 37°C.

2.3.1. EXPERIMENTAL DESIGN

During the release it is essential that the membrane is fully immersed in the PBS solution allowing the diffusion of the drug in all directions and not only through the parts in contact with the release medium. Thus, a glass vial was modified in order to keep the membrane submerge as shown in Figure 2.2. The experiment was conducted by placing the membranes in 5mL of PBS solution under agitation for 48h. At specific time points, the solution was completely collected and stored at 4°C and replaced by fresh PBS solution. The samples were taken every hour during the first 6h and then at 8h, 24h and 48h time points. The stored samples were next analysed by UV/Vis-spectroscopy for IBU quantification. All experiments were conducted in triplicate. The spectrophotometer used was a Shimadzu UV-Visible 2401 PC and a new calibration curve was prepared as previously described, yielding an $R^2=1$ and the equation $Y = 1.6005X+0.0008$.



Figure 2.2: Disassembled (left) and assembled (right) modified glass vial used in drug release assays, with a submerged membrane (red rectangle).

2.3.2. RELEASE ASSAYS UNDER MAGNETIC FIELD

In order to understand the influence of the Terfenol-D particles in the release profile, the final experiment was conducted under magnetic fields. The magnetic fields was applied in the first 8h of the assay. During the first hour no magnetic field was applied for two reasons. The first reason was the necessity to have a comparable value to match the assay without an applied field in order to validate the results. The

second reason was the time needed for the drug to exit the zeolite towards the polymeric matrix. The field was applied by a home-made setup with an applied AC field of 0.3Hz of frequency from 0 to 0.2T.

2.3.3. DRUG RELEASE MATHEMATICAL MODELS

When studying drug release profiles it is important to better understand how the release occurs and of how it is being controlled. Therefore, some mathematical models are used to reach some conclusions. The most widely used are the zero-order and first-order models, the Higuchi model and the Korsmeyer-Peppas model. In Table 2.1 are summarized the equations of each model and how to plot the obtained results in order to fit the models.

Table 2.1 – Drug release mathematical models. From [71,72].

MODEL	EQUATION	PLOT
Zero-order	$Q_t = Q_0 + K_0 t$	Cumulative drug release vs. time
First-order	$\log C = \log C_0 - \frac{K_1 t}{2.303}$	Log cumulative percentage of drug remaining vs. time
Higuchi	$\frac{M_t}{M_\infty} = K_H \sqrt{t}$	Cumulative percentage of drug released vs. square root of time
Korsmeyer-Peppas	$\frac{M_t}{M_\infty} = K t^n$	Log cumulative percentage of drug released vs. log time

Keys: Q_t is the amount of drug dissolved in time t ; Q_0 is the initial amount of drug in the solution; K_0 is the zero order release constant; C is the calculated concentration; C_0 is the initial concentration of drug; K_1 is the first order release constant; M_t/M_∞ is a fraction of drug released at time t ; K_H is the Higuchi dissolution constant; K is the release rate constant and n is the release exponent.

A zero-order release kinetic indicates that the release rate is independent of time [72], whereas a first-order kinetic specifies that the release rate is dependent of the concentration of drug still remaining inside the platform [73]. The Higuchi model was the first mathematical model to explain the release of a drug from a matrix system. Due to the extreme simplicity of its equation, Higuchi's model is one of the most used models and, even though it contains six important assumptions [71] that are rarely fully verified in drug delivery systems (initial drug concentration in the matrix is much higher than drug solubility; drug diffusion takes place only in one dimension (edge effect must be negligible); drug particles are much smaller than system thickness; matrix swelling and dissolution are negligible; drug diffusivity is constant; and perfect sink conditions are always attained in the release environment), it can still provide a rough

idea of the primary release mechanism [72]. Lastly, the Korsmeyer-Peppas model described the drug release from polymeric systems. This model can provide information allowing to distinguish between different release mechanisms. In Table 2.2 are summarized the n values of the Korsmeyer-Peppas model and the associated release mechanisms.

Table 2.2 – Exponent n of the Korsmeyer-Peppas model and drug release mechanism from cylindrical polymeric drug release systems. Adapted from [71,72].

EXPONENT, n	DRUG RELEASE MECHANISM
0.45	Fickian diffusion
$0.45 < n < 0.89$	Anomalous transport
0.89	Case-II transport (zero-order)
> 0.89	Super Case-II transport

2.4. CHARACTERIZATION TECHNIQUES

2.4.1. SCANNING ELECTRON MICROSCOPY

Aiming to study the membrane's pore system, Scanning electron microscopy (SEM) was the chosen imaging technique. The information provided by the secondary electrons (SE) and the backscattered electrons (BSE) allows the visualization of sample with different outputs. The SE, which are generated from the sample's surface (500-2000nm in depth) provide topographic information, with a resolution between 1-10nm. On the other hand, the most important information provided by BSE is related with the backscattered coefficient dependence on the atomic number (Z) [74]. This allows phases with different atomic numbers to be recognized, generating contrast if elements with different Z are present.

During this work, the microscope used was a JEOL-JSM-6300 in SE and BSE modes. To enable the visualization of the membrane's pore system, the samples were freeze-fractured in liquid nitrogen. Prior to the analysis, a thin gold layer was deposited in the samples to increase the conductivity, thus preventing the formation of static electric fields during the electron irradiation which would interfere with the acquired data

2.4.2. DIFFERENTIAL SCANNING CALORIMETRY

Differential scanning calorimetry (DSC) is a calorimetric technique used to measure thermal properties of a material, determining the temperature and heat flow associated with phase transitions as a function of time and temperature. During the analysis, the calorimeter measures the heat that is radiated or absorbed (exothermic or endothermic process, respectively) by the sample, comparing to a reference

material. This technique is useful to understand if the processing of the film or membrane will affect the polymer's characteristics, by detecting changes in the crystallization or fusion peaks.

The DSC system used during this work was a heat-flux DSC, from Perkin–Elmer, model Pyris-1 acquiring data from 30-200°C with a heating rate of 10°C/min. The samples were cut in small pieces and placed into 40µL aluminium pans.

2.4.3. THERMO-GRAVIMETRIC ANALYSIS

Thermo-gravimetric analysis (TGA) is a technique based on the temperature-related mass loss. During the analysis, the sample is placed on a scale and while the temperature increases the mass is being registered and a plot of mass loss (%) vs. temperature is created. In this work, TGA allowed to understand how much drug was incorporated in the zeolite and compare them with the other techniques used.

A thermobalance TG 209 F1 Libra® was utilized. In the method used the samples were heated up to 40°C followed by a 2min isothermal step. After that, the scanning was performed under a 60.0ml/min nitrogen flow up to 600°C and under an air flow of 60ml/min. up to 800°C, with a temperature ramp of 10°C/min. Before the procedure, the samples were kept at 70°C overnight to remove possibly adsorbed water. Higher temperatures would be necessary to remove water present inside the zeolitic lattice, however these temperatures could also cause alterations to the drug.

2.4.4. FOURIER-TRANSFORMED INFRARED SPECTROSCOPY

In order to confirm the presence of the drug in the zeolite, Fourier-transformed infrared (FTIR) spectroscopy was used. In infrared spectroscopy the sample is irradiated with infrared radiation aiming to identify specific vibrational behaviours. Knowing that the absorbed radiation's frequency will match the vibrational frequency of bonds and of functional groups of the present molecules, and that each bond presents characteristic vibrational frequencies, it is then possible to identify different molecules with distinctive functional groups. For these studies, a Bomem spectrophotometer was used and the analysis were conducted in the 4000-400cm⁻¹ range with a 4cm⁻¹ resolution in transmittance mode.

CHAPTER 3:

RESULTS AND DISCUSSION

3.1. THEORETICAL MODELLING OF IBU ENCAPSULATION.....	47
3.2. EXPERIMENTAL STUDIES OF IBUPROFEN ENCAPSULATION	50
3.2.1. FTIR STUDIES	51
3.2.2. THERMO-GRAVIMETRIC ANALYSIS.....	51
3.2.3. DRUG RELEASE PROFILES.....	52
3.3. POLY(L-LACTIC ACID) MEMBRANES PREPARATION	56
3.3.1. POLYMER CONCENTRATION OPTIMIZATION	56
3.3.2. RELEASE OF IBUPROFEN FROM THE PREPARED MEMBRANES	58
3.4. INCORPORATION OF THE ZEOLITE IN THE POLYMERIC MEMBRANES.....	59
3.5. PROOF OF CONCEPT – MAGNETICALLY MODULATED DRUG RELEASE	61
3.6. COMPARISON OF THE PREPARED DRUG RELEASE SYSTEMS	613

3.1. THEORETICAL MODELLING OF IBU ENCAPSULATION

During the first stage of the work, molecular modelling simulations were made in order to understand how the drug would interact with the carrier and how that could influence the loading and the diffusion. As mentioned, five structures were tested (FAU, BEA, MOR, MFI and FER) and are represented in Figure 3.1. In these representations it is possible to see an IBU molecule incorporated in a pore. Also, in some cases, namely with MOR, MFI and FER, it is possible to see purple dotted lines which represent close contacts between the drug and the zeolite, i.e. particular places where interactions occur, such as van der Waals or electrostatic interactions. From Figure 3.1 it is also possible to observe that not all pores are of the same size, also the different amount of interactions occurring in different structures. FAU, BEA and MOR present 12-membered ring channels, whereas MFI and FER present 10-membered rings. Both FAU and BEA present tridimensional main pore systems with interconnected channels and, in case of FAU, also with interconnected super-cages (Figure 3.2), while MOR presents a unidirectional pore system. MFI and FER present interconnected channels, but only in two directions.

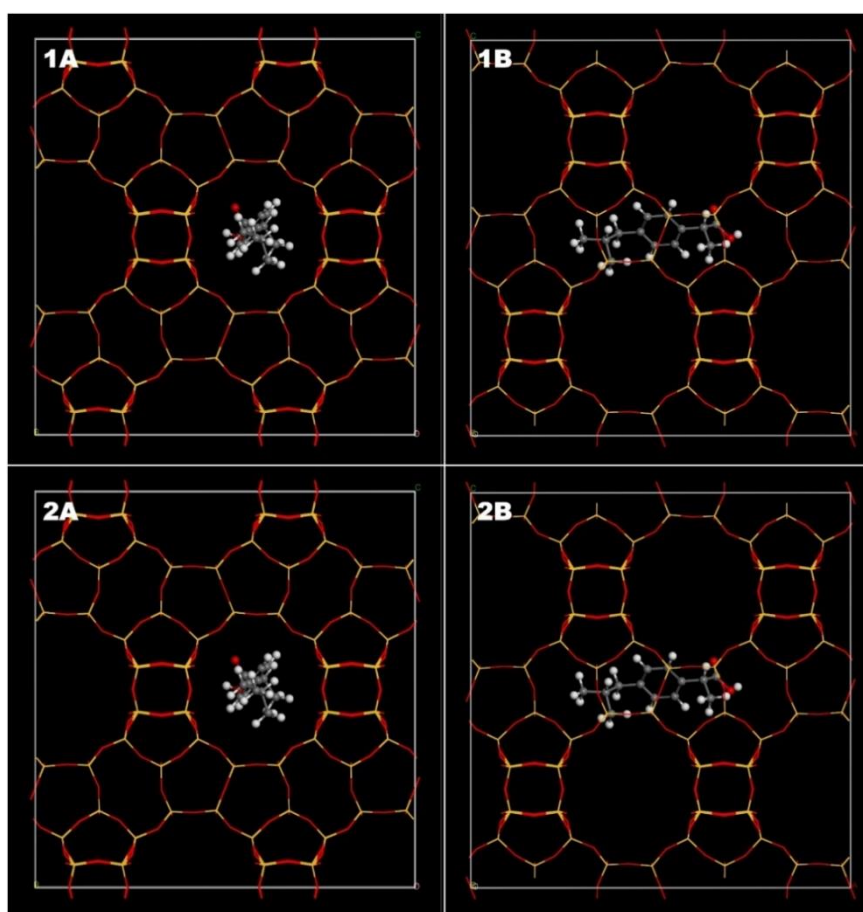


Figure 3.1: Zeolitic structures used in the theoretical modelling studies.

Keys: 1- Faujasite; 2 – Beta polymorph A. A – Front view; B – Side view.

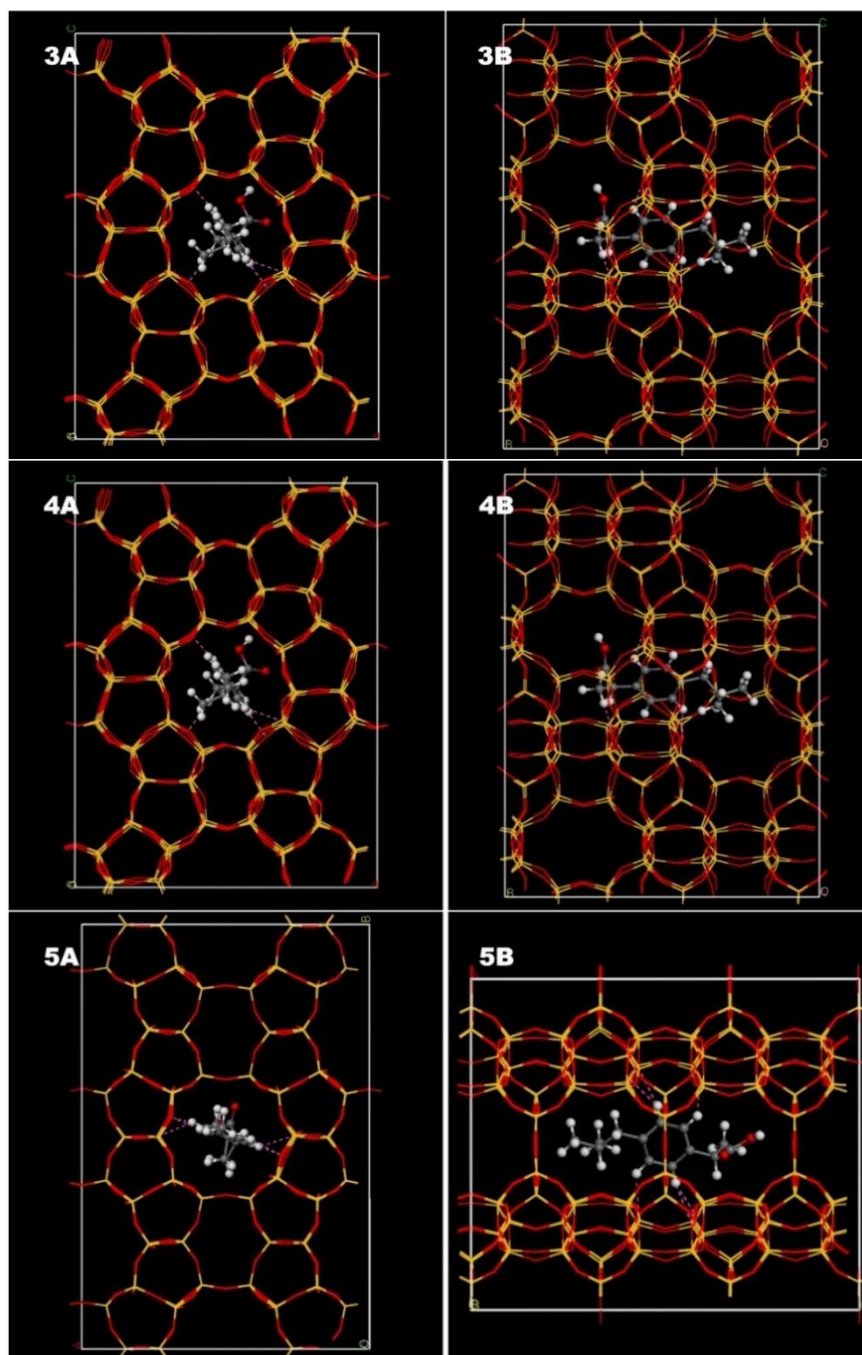


Figure 3.1 (continues): Zeolitic structures used in the theoretical modelling studies.
Keys: 3 – Mordenite; 4 – MFI; 5 – Ferrierite. A – Front view; B – Side view.

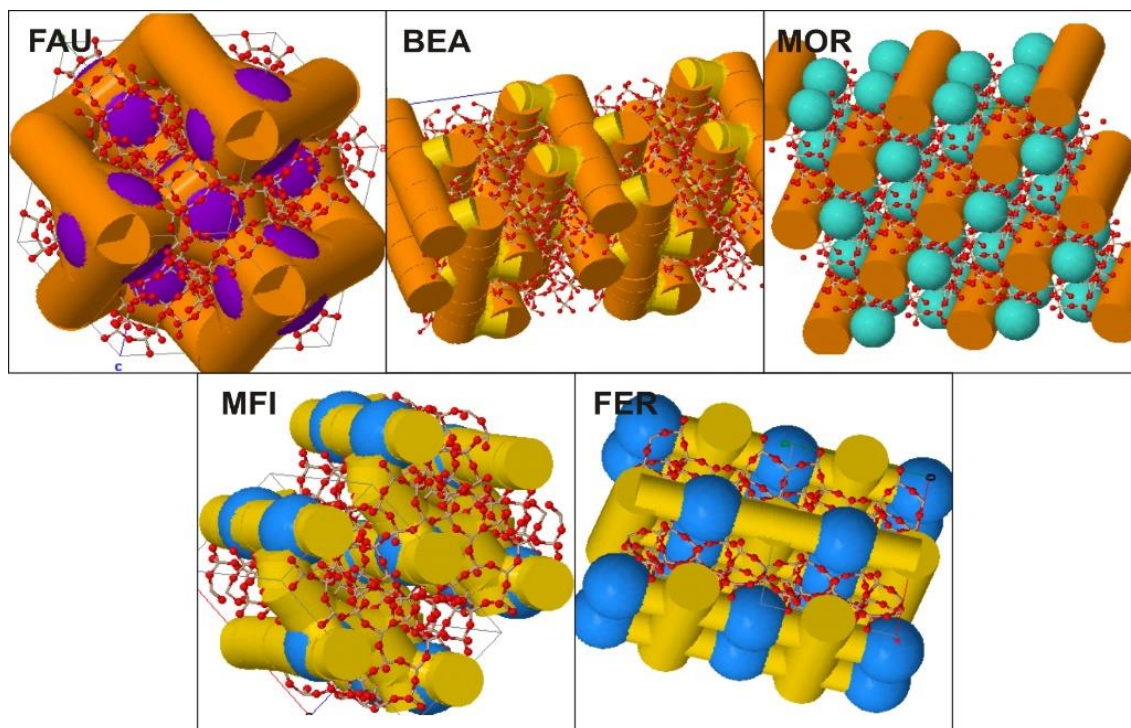


Figure 3.2: Structures of the studied zeolites. Only main pore frameworks are shown. Small pore systems with diameter $<4\text{\AA}$ are ignored due to negligible access by ibuprofen. From [18].

Keys: FAU – Faujasite; BEA – Beta polymorph alpha; MOR – Mordenite; MFI, Zeolite Socony Mobil-5; FER - Ferrierite. Orange pores – diameter $>6\text{\AA}$; Yellow pores – diameter $4-6\text{\AA}$; Purple spheres – cages with diameter $>8\text{\AA}$; Dark blue spheres – cages with diameter $=4-8\text{\AA}$; Light blue spheres – cages with diameter $<4\text{\AA}$.

After a first structural analysis, a dynamic simulation was performed in order to understand how much the drug would move inside the zeolite. Figure 3.3 shows the mean square displacement (MSD) of the IBU molecule over time. MSD is the common measurement of the extent of the motion of an object or, in this case, a molecule.

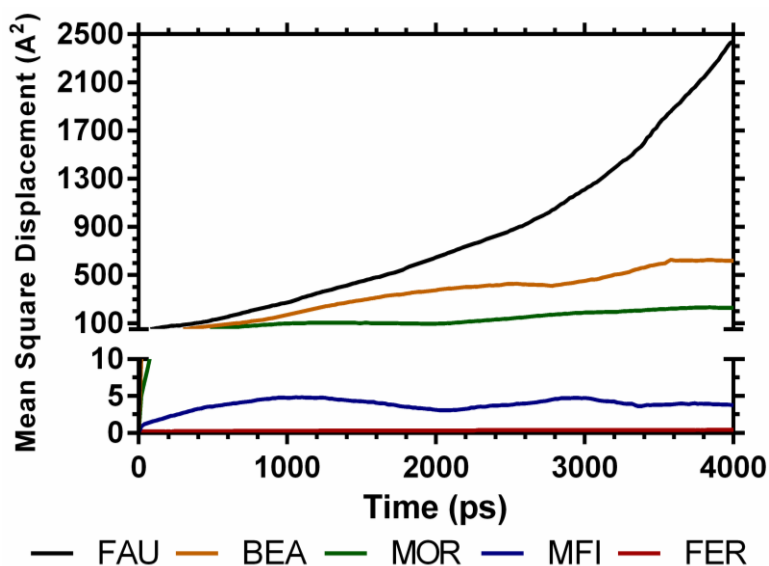


Figure 3.3: Mean Square Displacement of the Ibuprofen molecule in each zeolitic structure.

Keys: FAU – Faujasite; BEA – Beta polymorph alpha; MOR – Mordenite; MFI, Zeolite Socony Mobil-5; FER - Ferrierite

From the MSD data in Figure 3.3 is observable that FAU is the structure that offers the larger mobility to the IBU molecule, with MFI and FER showing negligible MSD. These results are explained by the differences in the zeolitic structures - not only the size of the pores but also the interconnections between channels. FAU presents a tridimensional pore system similarly to BEA, however it also presents interconnected super-cages (Figure 3.2), providing more freedom of movement. Also, even though BEA presents a tridimensional pore system, its main channel system is only in two perpendicular axes, with smaller channels interconnecting them (Figure 3.2). Both these reasons can help explain the difference of MSD concerning FAU and BEA. As mentioned, MOR presents a pore size identical to FAU and BEA (12-membered ring), however its channels are only oriented in one direction, alas the decreased MSD values compared to the other two structures. Finally, MFI and FER show unimportant values of MSD, mostly due to the decreased diameter of its channels (Figure 3.2) which originates close contacts between the zeolite and the drug (Figure 3.1).

3.2. EXPERIMENTAL STUDIES OF IBUPROFEN ENCAPSULATION

Following the molecular modelling results, experimental trials were conducted. The more exhaustively studied structure was FAU, since it was the one that presented the highest values of displacement. With this structure, five different zeolites with different counter-ions and different Si/Al ratios were tested and their release profiles and drug loading were assessed. Also, two BEA zeolites were tested. MOR, MFI and FER were included to confirm the outputs of the theoretical predictions. All the tested zeolites are summarized in Table 3.1. FAU samples were soaked in Act, EtOH and Hex to test the influence of the solvent. The other samples were only soaked in Hex.

Table 3.1 – Zeolites tested during the optimization stage.

STRUCTURE	COUNTER-ION	SI/AL RATIO
FAU	H ⁺	5.1
	H ⁺	80
	Na ⁺	5.1
	Na ⁺ (nano)	5.1
	NH ₄ ⁺	5.1
BEA	H ⁺	28
	NH ₄ ⁺	360
MOR	NH ₄ ⁺	20
MFI	NH ₄ ⁺	23
FER	NH ₄ ⁺	20

Keys: FAU – Faujasite; BEA – Beta polymorph alpha; MOR – Mordenite; MFI – Zeolite Socony Mobil-5; FER – Ferrierite.

3.2.1. FTIR STUDIES

Following the incorporation of the IBU in the zeolite, FTIR studies were performed in order to characterise the system and also to confirm the presence of the drug. Figure 3.4 shows the FTIR spectra of the zeolite, of the drug and of the IBU loaded zeolite. Peaks 1 and 3 (at 2951 cm^{-1} and at 1721 cm^{-1} , respectively) are representative of the $-\text{COOH}$ moiety of IBU, with peak 1 corresponding the $(-\text{OH})$ stretching and peak 3 the $(\text{C}=\text{O})$ stretching [75]. On the other hand, peak 4 (at 1640 cm^{-1}) is related to the zeolitic structure, corresponding to the $(\text{H}-\text{O}-\text{H})$ bending vibrations of the water molecules present in the structure [76,77]. Peaks 2 and 6 correspond to C-H stretching and bending vibrations and peak 5 to the aromatic ring $(\text{C}=\text{C})$ stretching vibration.

Thus, the existence of the selected peaks in the loaded zeolite samples indicates the presence of the drug in the sample. It is not possible to indicate if the drug is inside the zeolitic pores or present at the surface, however is possible to affirm that it is conjugated with the zeolitic structure.

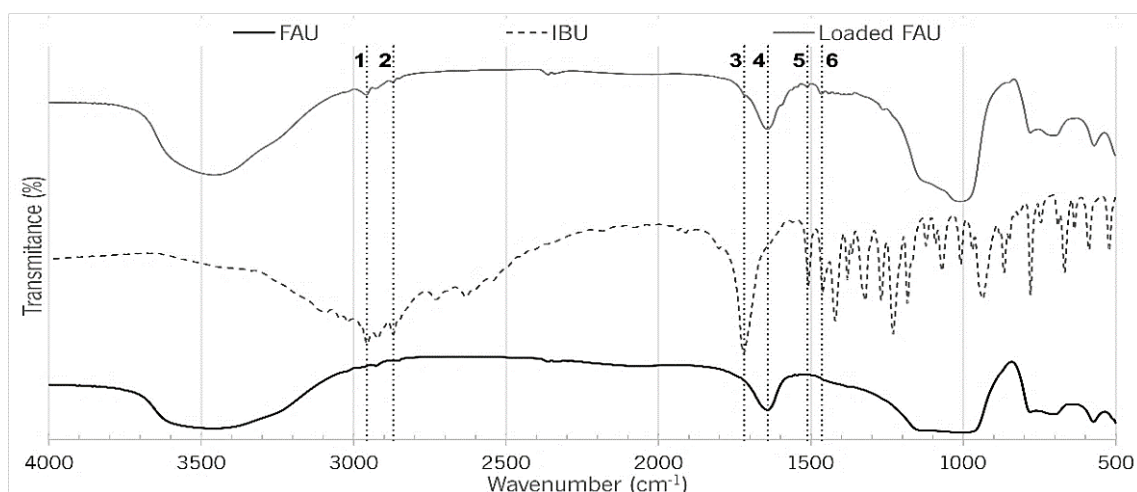


Figure 3.4: FTIR spectra of the zeolite, the drug and drug loaded carrier.

Keys: FAU – Faujasite structure; IBU – Ibuprofen.

3.2.2. THERMO-GRAVIMETRIC ANALYSIS

The loaded zeolites were then subject to a thermos-gravimetric analysis (TGA) in order to try to assess the amount of drug present in the samples. The results obtained from these studies are summarized in Table 3.2 and Figure 3.5 shows an example of the obtained data.

From Figure 3.5 is possible to see a first mass loss up until nearly 200°C This first mass loss can be attributed mainly to the remaining solvents or water present in the zeolitic structure [8]. The following step corresponds to the mass loss of the drug. At 600°C the nitrogen flow is replaced by an air flow, which, due to the presence of oxygen, will allow the full combustion of any organics present in the sample.

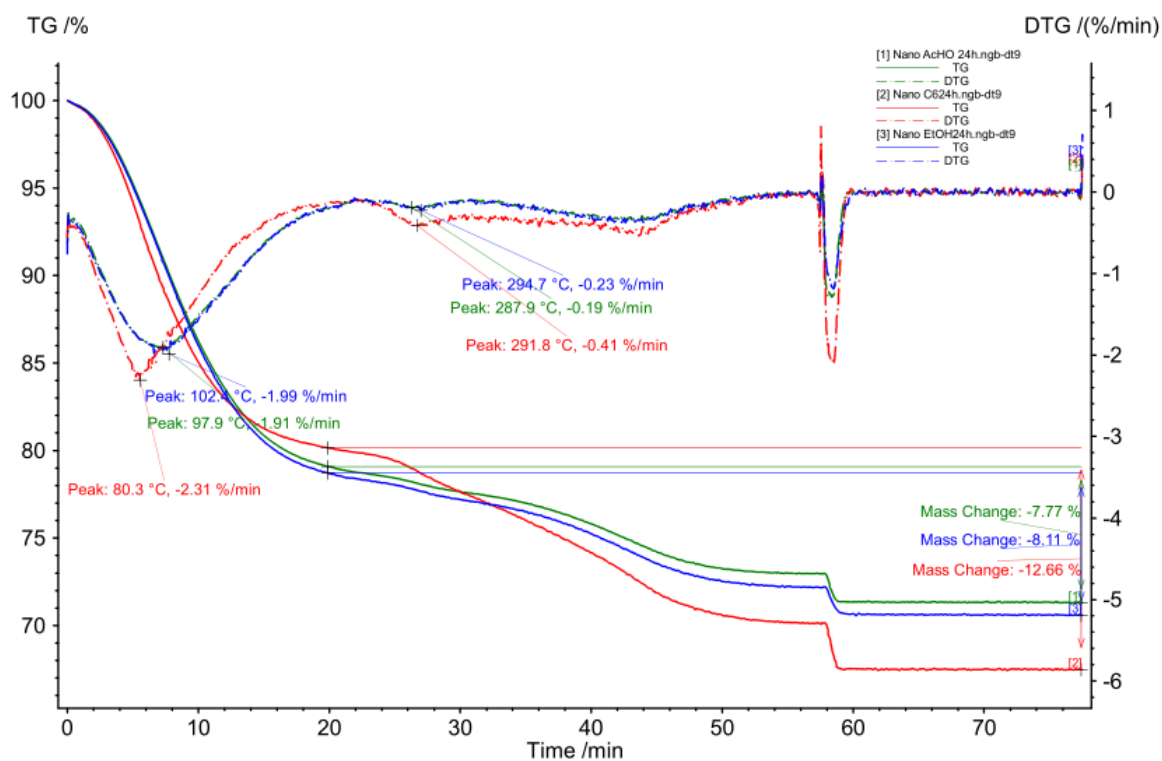


Figure 3.5: Thermo-gravimetric analysis of nano-FAU zeolites loaded with ibuprofen using different solvents. Starting temperature: 40°C; step: 10°/min.

Keys: FAU – Faujasite; Green lines – Acetone; Blue lines – Ethanol; Redlines – Hexane; solid lines – thermogram; dashed lines – first derivative.

In these studies, it was not always easy to calculate the mass loss attributable to the drug, mostly due to the overlap between the temperatures when IBU starts decomposing and the temperature when the water present deep inside the zeolitic structure is still evaporating. However, even though some of the results in Table 3.2 may differ from the ones observed in the release studies, the trend throughout the samples remains similar.

3.2.3. DRUG RELEASE PROFILES

In Figures 3.6, 3.7, 3.8 and 3.9 are represented the release profiles of IBU from the different tested zeolites and Table 3.2 summarizes the calculated drug loadings for all samples.

3.2.3.1. INFLUENCE OF THE LOADING SOLVENT

In a first analysis, it is observable that samples that were loaded using a hexane as solvent present the highest loading values – Figures 3.6 and 3.7 show the example of Na⁺-forms of FAU, however the same trend is observed in all other samples (Table 3.2). The different values obtained with the solvents may be explained by their chemical characteristics. Hexane has no functional groups, is non-polar and no reaction should occur with IBU. On the other hand, methanol, presents a hydroxyl group and acetone

presents a carbonyl. Both these groups can directly interact with the IBU molecule or even with the zeolite, hampering the incorporation of the drug into the zeolitic structure.

Table 3.2 – Drug loading of all tested samples of zeolites.

Structure	Counter-ion	Si/Al ratio	Solvent	Loading (%) ^a	Loading (%) ^b	
FAU	H ⁺	5.1	Hexane	9.9	13.6	
			Ethanol	8.1	10.5	
			Acetone	6.3	8.2	
		80	Hexane	17.4	16.2	
			Ethanol	13.2	16.1	
			Acetone	7.4	15.9	
	Na ⁺	5.1	Hexane	10.6	6.9	
			Ethanol	8.1	4.1	
			Acetone	7.6	4.5	
		Na ⁺ (nano)	5.1	Hexane	17.8	12.7
				Ethanol	9.3	8.1
				Acetone	9.3	7.8
NH ₄ ⁺	5.1	Hexane	27.3	11.6		
		Ethanol	21.1	12.2		
		Acetone	19.2	11.9		
	BEA	H ⁺	28		40.7	15.3
		NH ₄ ⁺	360		22.9	16.6
	MOR	NH ₄ ⁺	20	Hexane	26.3	-
MFI	NH ₄ ⁺	23		11.9	-	
FER	NH ₄ ⁺	20		12.6	-	

Keys: FAU – Faujasite; BEA – Beta polymorph alpha; MOR – Mordenite; MFI – Zeolite Socony Mobil-5; FER – Ferrierite. a – assessed by amount of drug released; b – assessed by thermo-gravimetric analysis.

3.2.3.2. CRYSTAL SIZE INFLUENCE

As for the influence of the size of the crystal, Nano FAU samples (FAU crystals with ~250nm in diameter) present greater IBU loading than the regular FAU crystals, with no specified size (figure 3.6 and 3.7, respectively). Furthermore, not only the loaded amount of drug seems different, but also the release profile. Nano FAU samples (Figure 3.6) release almost all content at around 24h, whereas regular FAU samples (Figure 3.7) present a more prolonged release, lasting in some cases up to 48h. With larger the crystals it takes longer for the releasing media to fill the zeolitic pores and also the longer the path the drug has to travel until it is released from inside the zeolite.

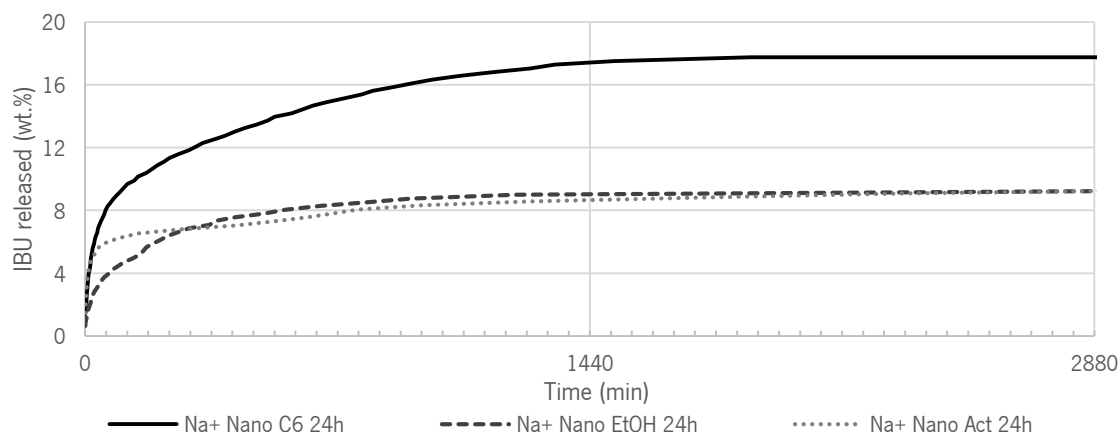


Figure 3.6: Ibuprofen (IBU) release from nanosized Na⁺-form faujasite with a 5.1 Si/Al ratio. Hexane (C6), ethanol (EtOH) and acetone (Act) were used as loading solvents. Minor tick marks in horizontal axis represent 1 hour.

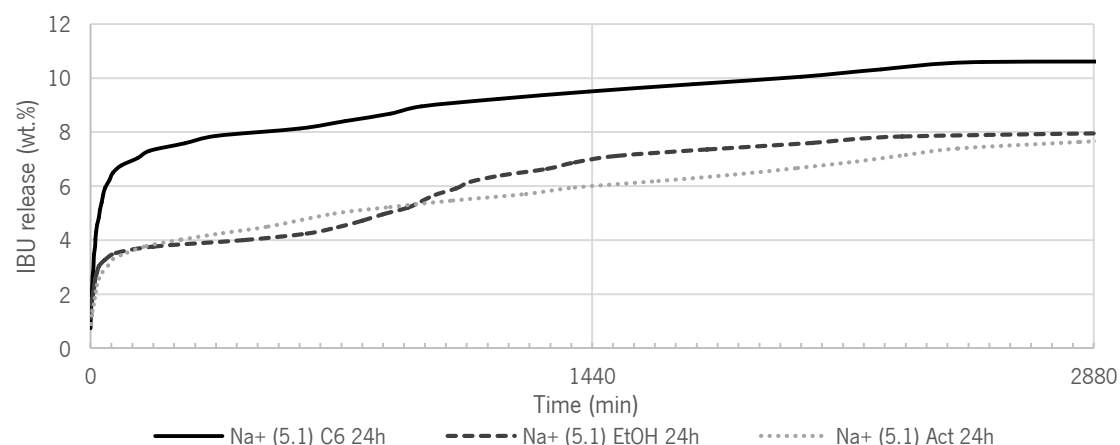


Figure 3.7: Ibuprofen (IBU) release from Na⁺-form Faujasite with a 5.1 Si/Al ratio. Hexane (C6), ethanol (EtOH) and acetone (Act) were used as loading solvents. Minor tick marks in horizontal axis represent 1 hour.

3.2.3.3. EFFECT OF THE COUNTER-ION AND Si/Al RATIO

Considering the effect of the counter-ion, FAU samples in the NH₄⁺-form always presented the highest loadings, despite of the solvent used (Table 3.2). However, BEA with H⁺ as counter-ion and a Si/Al ratio of 360 presents the highest value of loading for all the studied samples. Thus, adding to the counter-ion effect, the influence of the Si/Al ratio also has to be considered. In Figure 3.8 is compared the influence of the counter-ion effect and Si/Al ratio in the release profile using FAU and BEA samples.

Firstly, as already mentioned, the sample of FAU with ammonia as counter-ion (FAU NH₄⁺ (5.1)) presents higher loading when comparing with the respective H⁺-form (FAU H⁺ (5.1)). Only the samples soaked in hexane are shown, however with the other solvents the trend is the same – higher loading when ammonia is the counter-ion (Table 3.2).

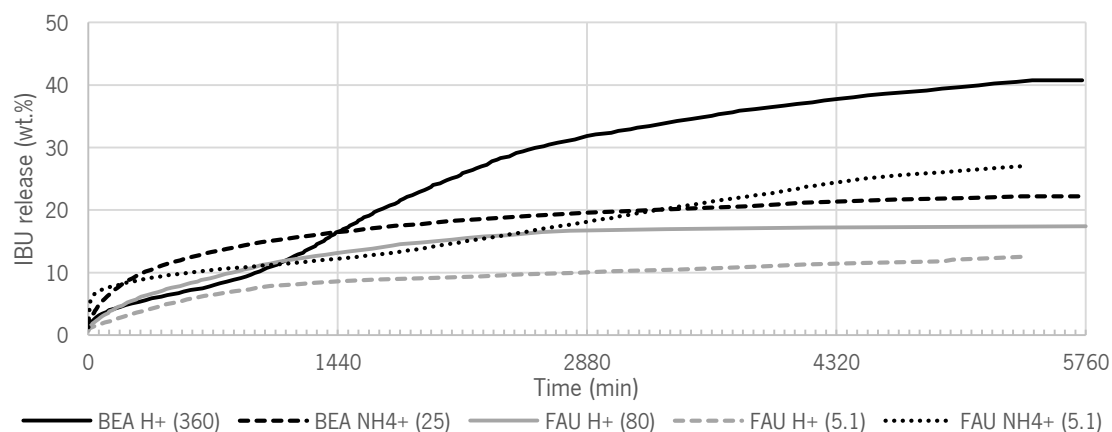


Figure 3.8: Ibuprofen (IBU) release from Beta polymorph alpha (BEA) and Faujasite (FAU) with different Si/Al ratios and counter-ions. Hexane was used as loading solvent. Minor tick marks in horizontal axis represent 1 hour.

Secondly, comparing the two presented H⁺-forms (FAU H⁺ (5.1) and FAU H⁺ (80)), it is observable that the structure with higher Si/Al ratio presents the highest loading. Again, this trend is observable with the other solvents as well (Table 3.2).

Lastly, when noticing the two BEA samples, it is clear that the one with the highest Si/Al ratio presents the highest loading, even though it is in its H⁺-form (contrarily to what was observed with FAU). In this case, it seems that the extremely high Si/Al ratio has the most influence in the drug loading. Being IBU a hydrophobic drug, higher Si/Al ratios (therefore higher hydrophobicity) seem to favour its loading onto the zeolitic pores. Unfortunately, there were no available BEA zeolites with Si/Al ratios comparable to the existing FAU samples, thus no definite conclusions can be drawn. However, it is clear that there both counter-ion and Si/Al ratio greatly influence the loading of the drug and that future work is needed to confirm these trends.

In order to confirm the molecular modelling predictions, another study was performed comparing the five studied structures (Figure 3.9). The only available counter-ion common to all structures was NH₄⁺, thus all studied structures are in this form. FAU, BEA and MOR present very similar drug loading, despite some differences in the release profile whereas FER and MFI present the lowest loading values.

These results were, in some extent, predicted by the theoretical simulations, especially for FER and MFI. All structures seem to present high loading values (above 10%), however this can be hypothesised to be influence of the counter ion and not the structure. Thus, this might indicate that the drug is not incorporated in the pores, but possibly only adsorbed to the surface of the crystal or interacting with the counter-ion, also causing a more delayed release.

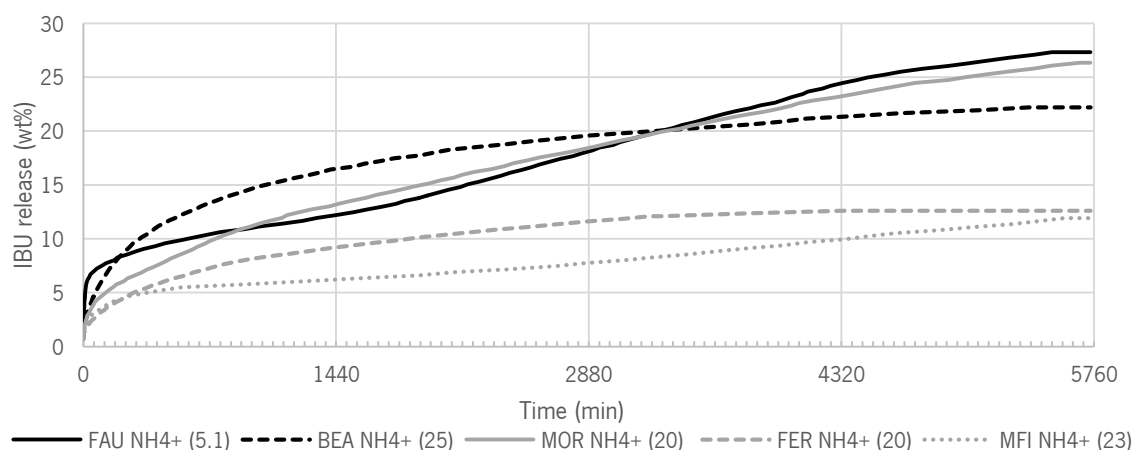


Figure 3.9: Ibuprofen (IBU) release from different zeolitic structures with different Si/Al ratios. Hexane was used as loading solvent. Minor tick marks in horizontal axis represent 1 hour.

Keys: FAU – Faujasite; BEA – Beta polymorph alpha; MOR – Mordenite; MFI, Zeolite Socony Mobil-5; FER – Ferrierite.

Considering the above release assays, the Nano FAU zeolite was chosen to continue the studies. This was done due to the release time shown by this sample. After nearly 24h this sample had completely release the drug, whereas in the other cases this happened after 48h, or in some cases even more. This choice was important because in the following release assays the dissolution apparatus was not available and experiments longer than 72h were not possible due to equipment limitations. Since the zeolite was to be integrated in a polymeric membrane a delay in the release time was expected, thus zeolites with longer release time may not have enough time to completely release the drug.

3.3. POLY(L-LACTIC ACID) MEMBRANES PREPARATION

3.3.1. POLYMER CONCENTRATION OPTIMIZATION

During the preliminary steps of the preparation of PLLA membranes, different polymer concentrations were tested. The membranes were prepared with 1, 3, 5 and 10(wt/vol.)% of polymer and were characterized by SEM (Figure 3.10) and DSC (Figure 3.11).

3.3.1.1. SCANNING ELECTRON MICROSCOPY

The 1(wt/vol.)% membrane showed not to have enough amount of polymer to form a stable membrane with the volume of solvent used. After the freeze drying process, all membranes prepared with this concentration presented fractures and incomplete formation of a uniform surface. As previously mentioned, the glass vials used to cast the solvent were 2.3cm in diameter and with 1mL of solution used, the membranes would have, in theory, a thickness of approx. 3mm. The theoretical superficial area of this membrane would be about 10cm². The polymer present in the solution with 1(wt/vol.)% was not

sufficient to form a membrane with these proportions, due to the polymer chains being too detached from each other, causing incomplete surface formation. The pore structure of the remaining three samples was studied by SEM and the respective results are presented in Figure 3.10.

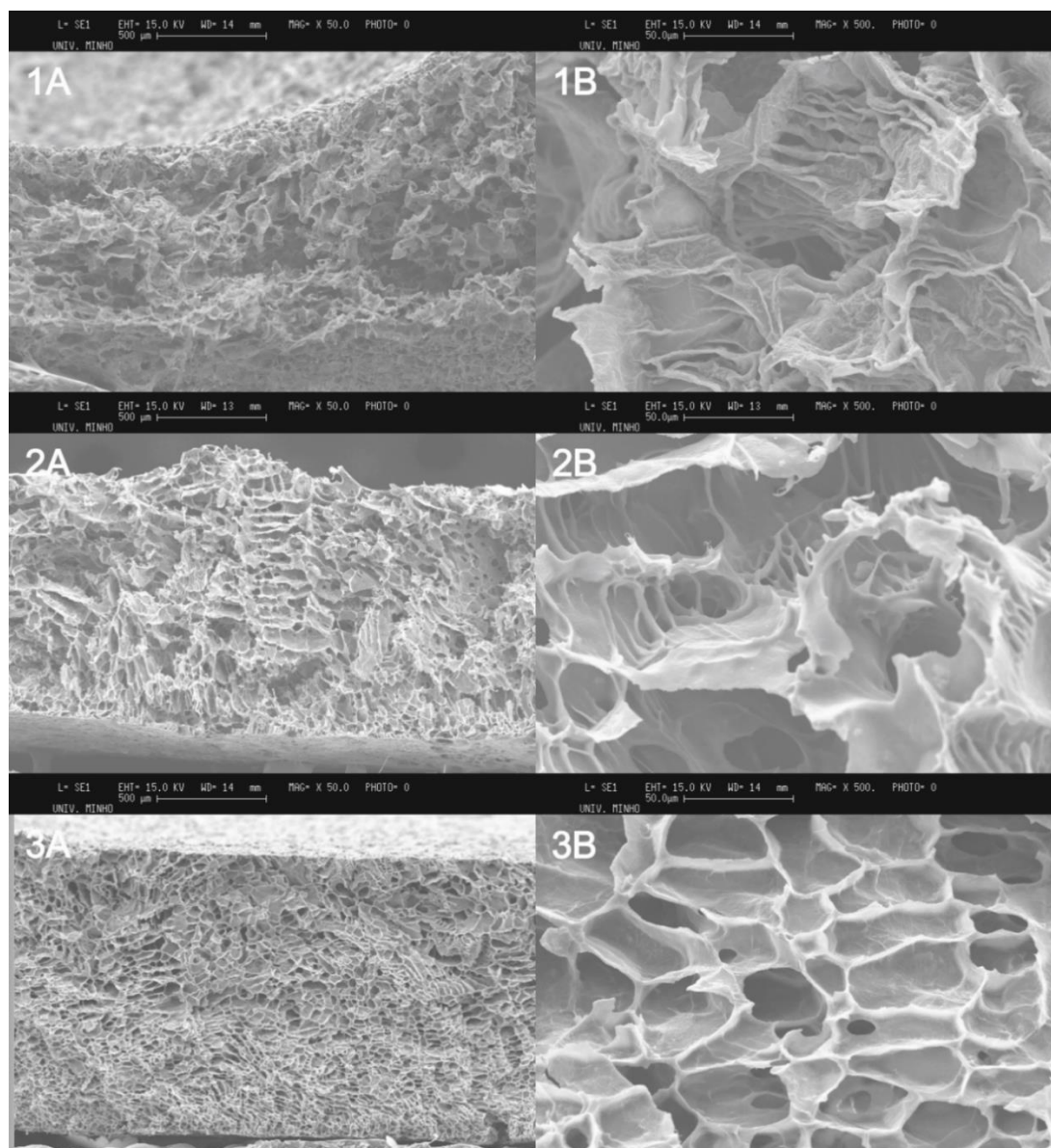


Figure 3.10: Scanning electron micrographs of poly(L-lactic acid) (PLLA) membranes.

Keys: 1 – 3(wt/vol.)% PLLA; 2 – 5(wt/vol.)% PLLA; 3 – 10(wt/vol.)% PLLA; A – 50x magnification; B – 500x magnification.

Sample 1, a 3(wt/vol.)% PLLA membrane, shows what seems to be deformed or collapsed pores, possibly present due to the insufficient amount of polymer during the preparation of the membrane. Contrarily to the 1% PLLA sample, 3(wt/vol.)% of polymer appears to be enough polymer to form a complete membrane, however it is still not enough to form stable pores. Macroscopically, this membrane showed to be very soft and excessively malleable. In sample 2, a 5(wt/vol.)% PLLA membrane, is possible

to observe a more defined pore system when compared to sample 1. This appeared to be the best concentration, as macroscopically the membrane showed to be malleable but, nevertheless, firm. As for sample 3, a 10(wt/vol.)% PLLA membrane, this membrane displays the smallest pores in all samples. Macroscopically, this was the most rigid membrane, presenting low malleability and being easily breakable when pressure was applied. Therefore, 5(wt/vol.)% of polymer was the chosen concentration to continue the studies.

3.3.1.2. DIFFERENTIAL SCANNING CALORIMETRY

Moreover, in order to assure that the polymer maintained its characteristics during the processing of the membranes, a DSC study was performed and the thermogram is represented in Figure 3.11.

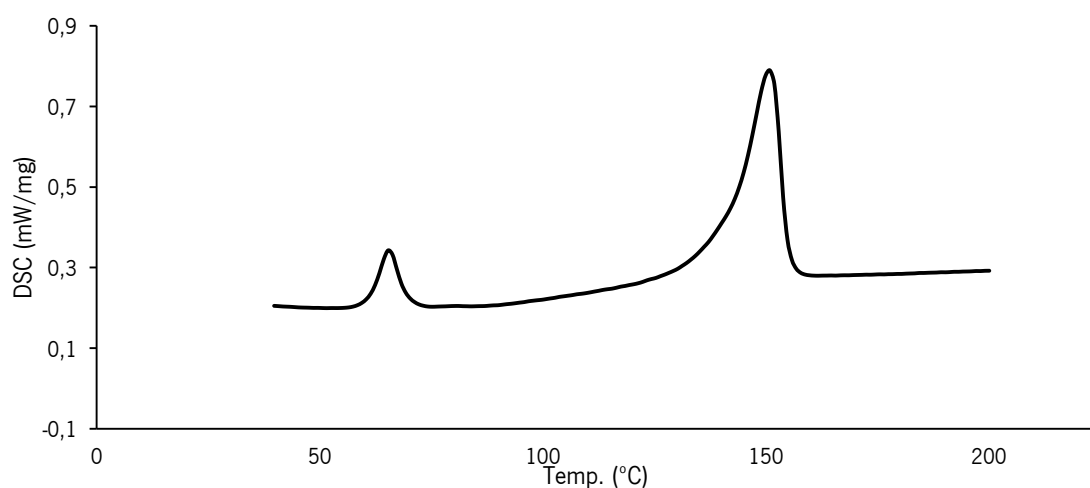


Figure 3.11: Differential scanning calorimetry thermogram of the prepared poly(L-lactic acid) membranes.

When comparing to other studies using PLLA from the same supplier [78], the produced membranes present similar DSC results. A first peak around 65°C is observable and corresponds to the glass transition of the polymer. A second endothermic peak is then detected at around 150°C, which corresponds to the melting point of PLLA. Therefore, the processing of the polymer did not alter its characteristics.

3.3.2. RELEASE OF IBUPROFEN FROM THE PREPARED MEMBRANES

To study the release kinetics of IBU from the prepared membranes, three different amounts of drug were added to the polymer solution during the process – 3, 5 and 10wt% of IBU (Figure 3.12).

The three samples reveal a release kinetic with similar tendencies: a burst release up to 8h and a more sustained release after. Considering the observed deviations, similar results are observed for the three samples, with around 40% of the drug being released after 48h. The results reveal that, for the first

8h, the correlation coefficients were higher for the zero-order release model (Table 3.3) comparing to a first order release, revealing that the drug release was independent from the remaining drug in the carrier. When looking to the complete release assay, the model that best fits the release kinetics is the Higuchi model, confirming that the drug release mechanism is controlled by diffusion. However, since this system is a polymeric matrix, the release mechanism can be based on diffusion and also on erosion [73]. For that reason the Korsmeyer-Peppas model was also applied. In the studied samples the drug release mechanism presents as an anomalous transport ($0.45 < n < 0.89$), meaning that the release is controlled both by diffusion and polymer swelling effects [72].

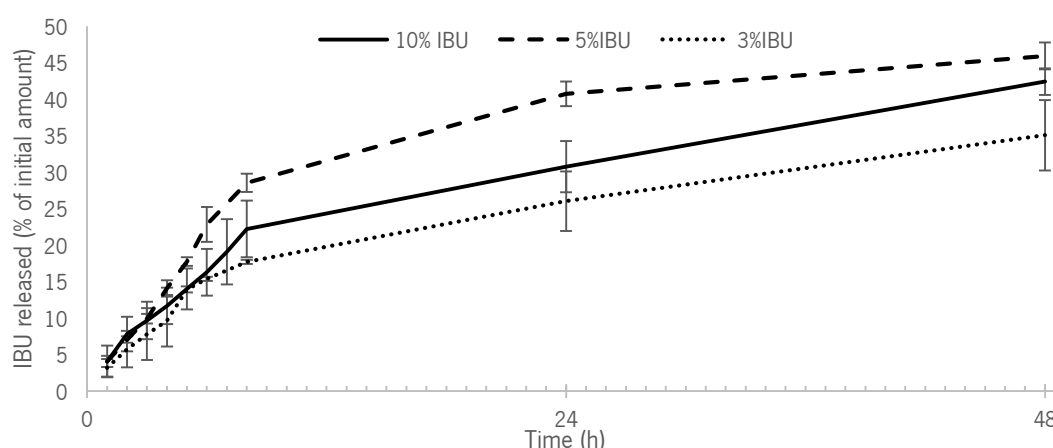


Figure 3.12: IBU release from PLLA membranes during 48 hours. Average \pm STD; $n=3$. **Key:** IBU - Ibuprofen

Table 3.3 – Release kinetics results from the tested ibuprofen (IBU)-loaded membranes.

Sample	Zero order	First order	Higuchi	Korsmeyer-Peppas	
	r^2	r^2	r^2	r^2	n
First 8h					
3% IBU	0.97	0.8948	0.9742	0.9896	0.8557
5% IBU	0.9941	0.9913	0.9648	0.992	0.9602
10% IBU	0.9925	0.9744	0.9847	0.9987	0.7771
48h release					
3% IBU	0.8713	0.5919	0.9635	0.9391	0.6095
5% IBU	0.7752	0.8292	0.9072	0.9121	0.6466
10% IBU	0.9139	0.7826	0.9702	0.9146	0.5607

3.4. INCORPORATION OF THE ZEOLITE IN THE POLYMERIC MEMBRANES

After the selection of an adequate polymer concentration, different amounts of Nano FAU were incorporated in the membranes during its preparation. The final polymeric system may need to contain diverse amounts of incorporated zeolite, depending on how much drug is loaded in the zeolite and on the desired

amount to be released. Therefore, several zeolite concentrations were tested in order to assess the influence of the zeolite in the polymeric matrix. The prepared membranes contained a final PLLA:zeolite mass proportion of 20, 10, 6, 4 and 2:1. SEM micrographs of two chosen samples are presented in Figure 3.13. These membranes contain a PLLA:zeolite ratio of 6:1 (sample 1) and 2:1 (sample 2).

It is observable the difference in the amount of zeolite present in each membrane, with sample 2 showing an almost completely covered surface, whereas sample 1 still presents some areas without zeolite. Moreover, the presence of the zeolite in the surface of the polymeric matrix may be desirable, causing the drug to diffuse easily out of the carrier. It is yet possible to admit that some zeolite may be present within the polymeric matrix and not only in the surface. Concerning the membrane stability, both samples formed consistent membranes, with the desired malleability with no sign of added fragility due to the presence of the zeolite.

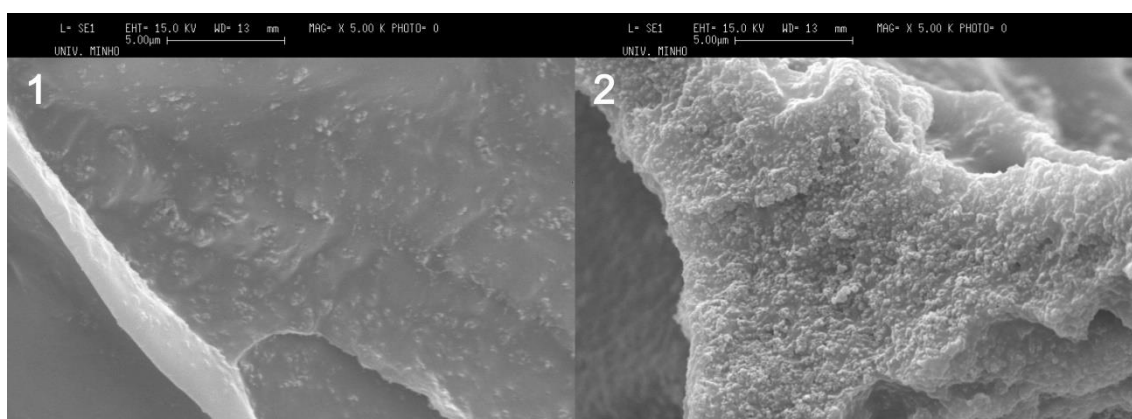


Figure 3.13: Scanning electron micrographs of 5 (wt/vol.)% poly(L-Lactic acid) (PLLA) membranes embedded with the nanosized faujasite zeolites.

Keys: 1 – PLLA:zeolite ratio = 6:1; 2 – PLLA:Zeolite ratio = 2:1

Moreover, to assure that the addition of the zeolite did not greatly influence the polymer structure, more DSC studies were conducted and are presented in Figure 3.14. The membrane containing the zeolite yielded a thermogram which contained the major peaks of the simple PLLA membranes. The broad peak around 100°C can be attributed to water present in the sample [79]. The zeolites easily absorb water from the surrounding environment and it is enough to be detected in a DSC analysis.

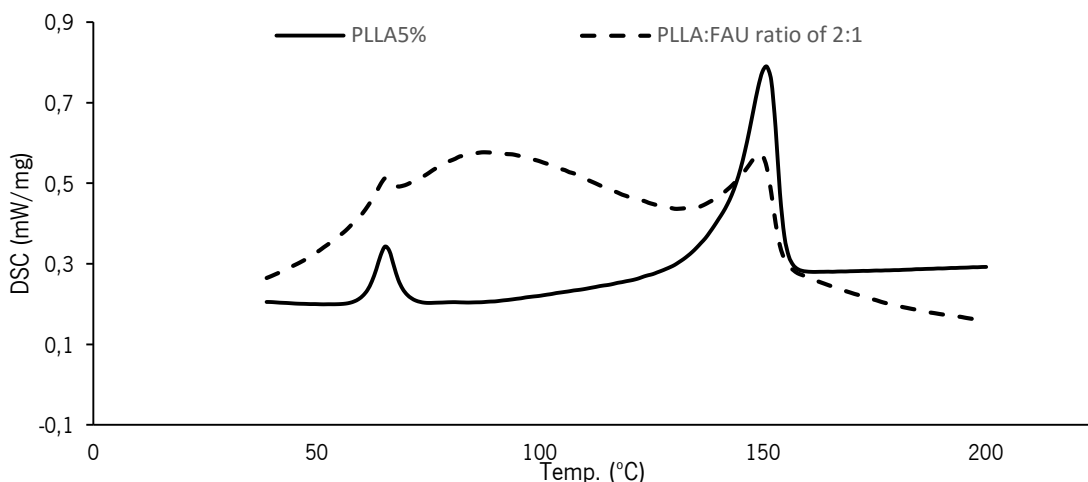


Figure 3.14: Differential scanning calorimetry thermogram of simple PLLA membranes and PLLA membranes containing zeolite (PLLA:FAU ratio of 2:1). **Key:** FAU – Faujasite; PLLA – Poly(L-lactic acid).

3.5. PROOF OF CONCEPT – MAGNETICALLY MODULATED DRUG RELEASE

After the incorporation of the zeolite in the polymeric membranes, the final step for the completion of the system was the integration of the magnetostrictive particles – Terfenol-D. These membranes were then subject to release assays in the presence and absence of magnetic fields in order to prove the modulation of the drug release. The release kinetics is shown in Figure 3.15 and the data from the fitting of the release models is summarized in Table 3.4.

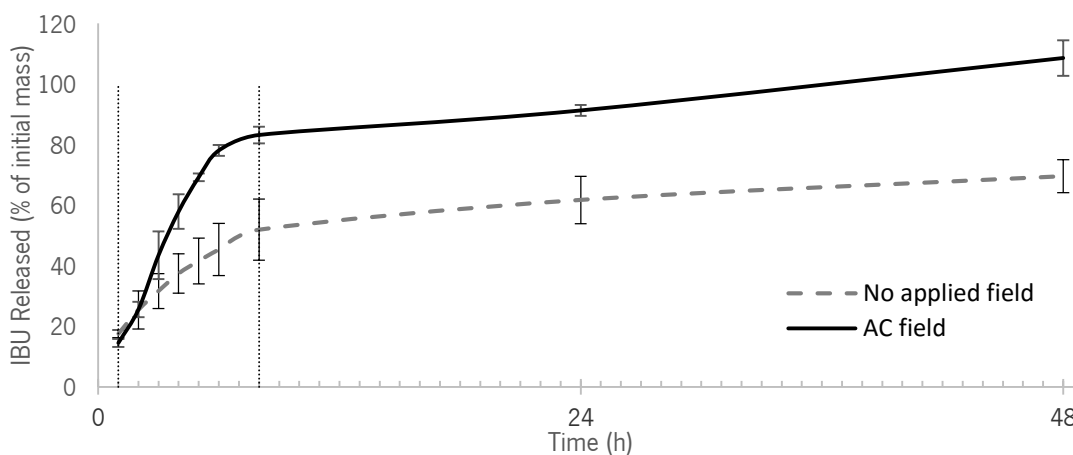


Figure 3.15: IBU release from PLLA membranes containing IBU-loaded FAU and Terfenol-D. One sample was subject to an AC field (0 to 0.2T) during the first 8h of the experiment (vertical lines). Average \pm STD; n=2. **Keys:** IBU – Ibuprofen.

Table 3.4 – Release kinetics results from the tested membranes containing IBU-loaded FAU and Terfenol-D.

Sample	Zero order	First order	Higuchi	Korsmeyer-Peppas	<i>n</i>
	r^2	r^2	r^2	r^2	
First 8h					
No field	0.9837	0.9993	0.9995	0.9998	0.5693
AC field	0.9298	0.9815	0.9727	0.9927	0.9789
48h release					
No field	0.7399	0.8406	0.872	0.9998	0.5693
AC field	0.5713	0.932	0.7281	0.9927	0.9789

Analysing the sample that was not subject to a magnetic field, it is possible to notice a burst release in the first 8h, reaching nearly 50% of the total amount of drug. After the 8h, a more sustained release is observed, with around 70% of the total drug being released after two days. This sample showed the best fitting with the first-order release kinetic (Table 3.4) in the first 8h, revealing a dependency with the residual concentration of drug. When no fields are applied, this membrane also presents a good correlation with the Higuchi model, indicating a diffusion-controlled process, which the Korsmeyer-Peppas model completes with the information an *n* of 0.56, indicating an anomalous diffusion (diffusion-controlled and swelling-driven release).

When the AC field is applied, a remarkable difference is observed: an increase in the release ratio. During the first 8h, when the magnetic field is turned on, a burst release occurs with around 80% of the drug being released, 30% more than without the magnetic field. Regarding the release models' fittings, again the Korsmeyer-Peppas model presents a very good fitting ($r^2=0.9927$), however the exponent *n* now presents a value higher than 0.89. This value indicates that the release mechanism is a super case-II transport, meaning that the release of the drug is being driven mostly by a swelling or erosion mechanism [72,73].

As formerly mentioned, when in presence of a magnetic field Terfenol-D will change its shape and size. When integrated in a polymeric membrane, these morphological changes will destabilise the polymeric matrix, possibly causing swelling in some locations or even rupture of some polymeric chains. This effect explains the observed results, justifying the transformation from an anomalous transport to a super case-II transport when magnetic fields are applied. Hence, when the membrane is under the influence of the magnetic field only a mechanism of swelling or erosion-controlled drug release is observed.

3.6. COMPARISON OF THE PREPARED DRUG RELEASE SYSTEMS

Throughout the work, four different drug release systems were prepared: IBU-loaded zeolites; IBU-loaded PLLA membranes; PLLA membranes containing loaded zeolites; and PLLA membranes containing loaded zeolites and Terfenol-D (released under the influence of magnetic fields). These four systems presented distinct release mechanisms and different release kinetics. The primary results are summarized in Table 3.5. Comparing the IBU release in all the produced systems, differences in the release kinetics are easily observed.

The release from IBU-loaded zeolites is well fitted to a first-order release when evaluating the 48h release ($r^2=0.9829$), meaning that the release is dependant of the amount of drug still present inside the carrier. This observation is further confirmed by the n exponent of the Korsmeyer-Peppas model ($n=0.3885$) which indicates a *quasi*-Fickian transport, meaning that the release is diffusion-controlled [72,80].

Analysing the release from IBU-loaded membranes, the best fitting for the release in the first 8h seems to be the zero-order release kinetic ($r^2=0.9941$), however for the 48h release this fitting is not appropriate. Regarding the Korsmeyer-Peppas n exponent for this sample, an anomalous release is identified, revealing that the release is diffusion guided but also influenced by the polymeric matrix's interaction with the solvent and consequent increase of its chains mobility [72].

As for the membranes containing IBU-loaded zeolites, the fitting of the release kinetics in the first 8h shows a first order release, similarly to the release from the IBU loaded zeolites. For longer periods of time, this type of kinetic is lost, but the n exponent indicates an anomalous transport, similarly to the IBU-loaded membranes. Thus, a hybrid type of release is observed for this platform.

Finally, when applying a magnetic field to the membranes containing IBU-loaded zeolites and Terfenol-D, the observed process is noticeably changed into a super case-II transport [71,72], with a good fitting with the Korsmeyer-Peppas model and an n exponent of 1.0117. This change, especially in the first 8h (when the fields are applied) from an anomalous release to a super case-II transport proves that the modifications in the polymeric matrix caused by Terfenol-D are now almost completely controlling the release.

Table 3.5 – Release kinetics results from the prepared drug release systems.

Sample	Zero order	First order	Higuchi	Korsmeyer-Peppas	
	r^2	r^2	r^2	r^2	n
First 8h					
IBU-loaded zeolite	0.7779	0.8985	0.9393	0.9828	0.3885
IBU-loaded PLLA membrane (5% IBU)	0.9941	0.9913	0.9648	0.992	0.9602
Membranes containing IBU-loaded zeolites	0.9837	0.9993	0.9995	0.9998	0.5693
Membranes containing IBU-loaded zeolites and Terfenol-D (AC field)	0.9298	0.9815	0.9727	0.9927	1.0117
48h release					
IBU-loaded zeolite	0.6328	0.9829	0.9398	-	-
IBU-loaded PLLA membrane (5% IBU)	0.7752	0.8292	0.9072	0.9121	0.6466
Membranes containing IBU-loaded zeolites	0.7399	0.8406	0.872	0.9998	0.5693
Membranes containing IBU-loaded zeolites and Terfenol-D (AC field)	0.5713	0.932	0.7281	-	-

Note: In order to be correctly fitted, Korsmeyer-Peppas model can only be applied until 60% of the drug is released [81], reason why in some cases the r^2 and the n exponent are not calculated.

CONCLUSIONS AND

FUTURE PERSPECTIVES

CONCLUSIONS

Nanomedicine and controllable drug delivery systems have recently initiated their way into therapeutics. Faulty and, many times, ineffective approaches that conventional medicine uses need to be replaced by novel and smart materials that assure that a drug is delivered in the right place, at the right time. Although several polymeric materials are currently being used to produce drug delivery systems it is, nevertheless, essential to reach an active control of the drug release rate. Therefore, the addition of a stimuli-sensitive component to the system that may trigger or increase the drug release rate would be of great interest. Also, since the use of zeolitic materials in drug delivery systems is relatively recent, it is important to understand the limitations of these materials and how certain characteristics of these aluminosilicates influence the loading of a drug. During this work, a polymeric platform containing a drug carrier (zeolite) and a stimuli-sensitive component (Terfenol-D) was produced.

Firstly, a theoretical and experimental screening involving different zeolites with different characteristics (structure, crystal size, Si/Al ratio and counter ion) and loading methods with different solvents (hexane, ethanol and acetone) was performed in order to understand their influence in the loading of a model drug – Ibuprofen.

Molecular modeling results showed that some structures, such as FER and MFI, are not able to fit the IBU molecule in their pores due to their smaller pores. In these studies, FAU and BEA showed to be the structures providing greater mobility to the drug, which could indicate a greater loading, but also a faster release. The experimental studies demonstrated that, even though the zeolitic structure is important to accommodate the guest molecule, other details also deserve careful analysis. The results showed that zeolites in the NH_4^+ -form always presented the highest drug loading comparing to the H^+ and Na^+ -form. Moreover, the solvent also revealed to be of great influence, with hexane providing the highest loadings for all structures. Lastly, the Si/Al ratio was also proven to directly influence the incorporation of the drug, with higher ratios yielding greater loading. Hence, when considering the incorporation of a drug in a zeolitic structure, all the characteristics should be carefully analyzed. For the subsequent studies, Nano FAU was the selected zeolite due to the presented release profile, with almost all its content being released in the first 24h. The release kinetics of this sample was perfectly fitted in a first order release ($r^2=0.9829$).

Regarding the preparation of the polymeric membranes, four different polymer concentrations were tested. The lowest concentration (1(wt/vol.))% was not able to form a complete membrane, possibly due to the lack of enough of polymer to form an interconnected matrix. The remaining three concentrations

CONCLUSIONS AND FUTURE PERSPECTIVES

(3, 5 and 10 (wt/vol.)) formed complete membranes, however the lowest concentration revealed collapsed pores in the SEM analysis and showed to be fragile. The other two samples presented stable interconnected pores, however the 5(wt/vol.)) sample was chosen to continue the studies, offering a membrane with good malleability and low fragility. Furthermore, the DSC studies showed that the processing of the membranes did not alter the polymer's characteristics.

The IBU-loaded membranes were prepared with three different drug concentration (3, 5 and 10 wt%). The release assays were performed in PBS at 37°C and in sink conditions for a period of 48h. Results exhibited a burst release in the first 8h for all the samples (with around 25% of the drug being released) and was fitted into a zero-order release kinetic. The n exponential of the Korsmeyer-Peppas model, revealed an anomalous transport, caused by diffusion and swelling-controlled release.

For the preparation of the complete platform containing both the loaded zeolites and Terfenol-D, a first study was done in order to test the stability of the membranes with high concentrations of the solids. DSC studies showed no alteration to the polymer when both particles were integrated. SEM confirmed the presence of the zeolite in the surface of the polymeric matrix and when a concentration of c.a. 33wt% of zeolite was used, the membrane remained stable and the surface fully covered with zeolitic material.

Preliminary results with membranes containing loaded zeolites and Terfenol-D were promising, demonstrating the effect of the magnetic field in the drug release ratio. Results showed that without the trigger an anomalous diffusion is observed, with an n exponential of 0.56. However, when a magnetic field is applied to the system the release mechanism is a super case-II transport, showing that the release of the drug is mainly controlled by swelling or erosion effects.

Comparing the four different drug release systems prepared (IBU-loaded zeolites; IBU-loaded PLLA membranes; PLLA membranes containing loaded zeolites; and PLLA membranes containing loaded zeolites and Terfenol-D (released under the influence of magnetic fields)) it is clear that the systems present significant differences in the release kinetics and mechanisms. The membranes containing IBU-loaded zeolites appear to present a combination between the release of IBU-loaded membranes and the IBU-loaded zeolites. On the other hand, when the system containing the loaded zeolites and Terfenol-D is under the influence of magnetic fields, the release mechanism is visibly a super case-II transport. As Terfenol-D is a magnetostrictive particle (i.e. changes its size and shape in presence of a magnetic field), the trigger will cause modifications to its morphology and, thus, to the polymeric matrix, increasing the release of the drug.

FUTURE PERSPECTIVES

More studies should be made regarding the influence of the mentioned characteristics of the zeolites in the loading of a drug. These investigations should be made with an increased number of tested samples since no systematic studies are found in the literature explaining how each feature influences the loading and the release of a drug.

Even though the results from the drug release under magnetic fields are only preliminary results, a proof of concept was obtained for these systems. Further tests need to be done with different fields, different intensities and different amounts of Terfenol-D (or even other magnetostrictive particles) in order to understand how tunable the drug release is. Following that idea, the use of these systems as drug release platforms or the incorporation in more complex system for the controlled release of substances will be a possibility.

REFERENCES

- [1] G. Vilar, J. Tulla-Puche, F. Albericio, Polymers and drug delivery systems, *Current Drug Delivery*. 9 (2012) 367–394. doi:10.2174/156720112801323053.
- [2] S. Ganta, H. Devalapally, A. Shahiwala, M. Amiji, A review of stimuli-responsive nanocarriers for drug and gene delivery, *Journal of Controlled Release*. 126 (2008) 187–204. doi:10.1016/j.jconrel.2007.12.017.
- [3] D. Roy, J.N. Cambre, B.S. Sumerlin, Future perspectives and recent advances in stimuli-responsive materials, *Progress in Polymer Science*. 35 (2010) 278–301. doi:10.1016/j.progpolymsci.2009.10.008.
- [4] A.S. Hoffman, Stimuli-responsive polymers: Biomedical applications and challenges for clinical translation, *Advanced Drug Delivery Reviews*. 65 (2013) 10–16. doi:10.1016/j.addr.2012.11.004.
- [5] S. Parveen, R. Misra, S.K. Sahoo, Nanoparticles: a boon to drug delivery, therapeutics, diagnostics and imaging, *Nanomedicine: Nanotechnology, Biology and Medicine*. 8 (2012) 147–166. doi:10.1016/j.nano.2011.05.016.
- [6] M.G. Rimoli, M.R. Rabaioli, D. Melisi, A. Curcio, S. Mondello, R. Mirabelli, et al., Synthetic zeolites as a new tool for drug delivery, *Journal of Biomedical Materials Research. Part A*. 87 (2008) 156–164. doi:10.1002/jbm.a.31763.
- [7] H. Eriksson, Controlled release of preservatives using dealuminated zeolite Y, *Journal of Biochemical and Biophysical Methods*. 70 (2008) 1139–1144. doi:10.1016/j.jbbm.2007.05.010.
- [8] P. Horcajada, C. Márquez-Alvarez, A. Rámila, J. Pérez-Pariente, M. Vallet-Regí, Controlled release of Ibuprofen from dealuminated faujasites, *Solid State Sciences*. 8 (2006) 1459–1465. doi:10.1016/j.solidstatesciences.2006.07.016.
- [9] R. Amorim, N. Vilaça, O. Martinho, R.M. Reis, M. Sardo, J. Rocha, et al., Zeolite Structures Loading with an Anticancer Compound As Drug Delivery Systems, *The Journal of Physical Chemistry C*. 116 (2012) 25642–25650. doi:10.1021/jp3093868.
- [10] I. Braschi, G. Gatti, G. Paul, C.E. Gessa, M. Cossi, L. Marchese, Sulfonamide Antibiotics Embedded in High Silica Zeolite Y: A Combined Experimental and Theoretical Study of Host–Guest and Guest–Guest Interactions, *Langmuir*. 26 (2010) 9524–9532. doi:10.1021/la9049132.
- [11] S. Sotoudeh, A. Barati, R. Davarnejad, M. Farahani, Antibiotic Release Process from Hydrogel Nano Zeolite Composites, *Middle-East Journal of Scientific Research*. 12 (2012) 392–396. doi:10.5829/idosi.mejsr.2012.12.3.1062.
- [12] T. Ceyhan, M. Tatlier, H. Akçakaya, In vitro evaluation of the use of zeolites as biomaterials: effects on simulated body fluid and two types of cells, *Journal of Materials Science: Materials in Medicine*. 18 (2007) 1557–1562. doi:10.1007/s10856-007-3049-y.
- [13] M. Kralj, K. Pavelic, Medicine on a small scale, *EMBO Reports*. 4 (2003) 1008–1012. doi:10.1038/sj.embor.7400017.
- [14] A. Corma, H. Garcia, Supramolecular Host-Guest Systems in Zeolites Prepared by Ship-in-a-Bottle Synthesis, *European Journal of Inorganic Chemistry*. 2004 (2004) 1143–1164. doi:10.1002/ejic.200300831.
- [15] D. Bougeard, K.S. Smirnov, Modelling studies of water in crystalline nanoporous aluminosilicates, *Physical Chemistry Chemical Physics*. 9 (2006) 226–245. doi:10.1039/B614463M.
- [16] D.G. Fatouros, D. Douroumis, V. Nikolakis, S. Ntais, A.M. Moschovi, V. Trivedi, et al., In vitro and in silico investigations of drug delivery via zeolite BEA, *Journal of Materials Chemistry*. 21 (2011) 7789. doi:10.1039/c1jm10204d.
- [17] A. Corma, M.J. Díaz-Cabañas, J. Martínez-Triguero, F. Rey, J. Rius, A large-cavity zeolite with wide pore windows and potential as an oil refining catalyst, *Nature*. 418 (2002) 514–517. doi:10.1038/nature00924.
- [18] E.L. First, C.E. Gounaris, J. Wei, C.A. Floudas, Computational characterization of zeolite porous networks: an automated approach, *Physical Chemistry Chemical Physics*. 13 (2011) 17339–17358. doi:10.1039/C1CP21731C.
- [19] C. Baerlocher, L.B. McCusker, Database of Zeolite Structures, Database of Zeolite Structures. (2007). <http://www.iza-structure.org/databases/> (accessed July 25, 2015).

REFERENCES

- [20] H. Zhang, Y. Kim, P.K. Dutta, Controlled release of paraquat from surface-modified zeolite Y, *Microporous and Mesoporous Materials*. 88 (2006) 312–318. doi:10.1016/j.micromeso.2005.09.026.
- [21] F. Gao, G. Zhu, Y. Chen, Y. Li, S. Qiu, Assembly of *p*-Nitroaniline Molecule in the Channel of Zeolite MFI Large Single Crystal for NLO Material, *The Journal of Physical Chemistry B*. 108 (2004) 3426–3430. doi:10.1021/jp036330y.
- [22] H. Salazar, A.C. Lima, A.C. Lopes, G. Botelho, S. Lanceros-Mendez, Poly(vinylidene fluoride-trifluoroethylene)/NAY zeolite hybrid membranes as a drug release platform applied to ibuprofen release, *Colloids and Surfaces A: Physicochemical and Engineering Aspects*. 469 (2015) 93–99. doi:10.1016/j.colsurfa.2014.12.064.
- [23] M.N. Chrétien, B. Shen, H. García, A.M. English, J.C. Scaiano, Ship-in-a-bottle synthesis of fluorescence-labeled nanoparticles: applications in cellular imaging, *Photochem. Photobiol.* 80 (2004) 434–437. doi:10.1562/0031-8655(2004)080<0434:SSOFNA>2.0.CO;2.
- [24] M. Salavati-Niasari, A. Sobhani, Ship-in-a-bottle synthesis, characterization and catalytic oxidation of cyclohexane by Host (nanopores of zeolite-Y)/guest (Mn(II), Co(II), Ni(II) and Cu(II) complexes of bis(salicylaldehyde)oxaloyldihydrazone) nanocomposite materials, *Journal of Molecular Catalysis A: Chemical*. 285 (2008) 58–67. doi:10.1016/j.molcata.2008.01.030.
- [25] M.S. Thabet, A.H. Ahmed, Ship-in-a-bottle synthesis and physicochemical studies on zeolite encapsulated Mn(II), Mn(III)-semicarbazone complexes: application in the heterogeneous hydroxylation of benzene, *Journal of Porous Materials*. 20 (2013) 319–330. doi:10.1007/s10934-012-9600-3.
- [26] D.R. Rolison, C.A. Bessel, Electrocatalysis and Charge-Transfer Reactions at Redox-Modified Zeolites, *Accounts of Chemical Research*. 33 (2000) 737–744. doi:10.1021/ar9701272.
- [27] S.H. Bossmann, N. Shahin, H.L. Thanh, A. Bonfill, M. Wörner, A.M. Braun, [FeII(bpy)3]2+/TiO2-Codoped Zeolites: Synthesis, Characterization, and First Application in Photocatalysis, *Chem-PhysChem*. 3 (2002) 401–407. doi:10.1002/1439-7641(20020517)3:5<401::AID-CPHC401>3.0.CO;2-7.
- [28] Z. Li, Use of surfactant-modified zeolite as fertilizer carriers to control nitrate release, *Microporous and Mesoporous Materials*. 61 (2003) 181–188. doi:10.1016/S1387-1811(03)00366-4.
- [29] E. Khodaverdi, R. Honarmandi, M. Alibolandi, R.R. Baygi, F. Hadizadeh, G. Zohuri, Evaluation of synthetic zeolites as oral delivery vehicle for anti-inflammatory drugs, *Iranian Journal of Basic Medical Sciences*. 17 (2014) 337–343.
- [30] A. Dyer, S. Morgan, P. Wells, C. Williams, The use of zeolites as slow release anthelmintic carriers, *Journal of Helminthology*. 74 (2000) 137–141. doi:http://dx.doi.org/10.1017/S0022149X00000184.
- [31] N. Vilaça, R. Amorim, O. Martinho, R.M. Reis, F. Baltazar, A.M. Fonseca, et al., Encapsulation of α -cyano-4-hydroxycinnamic acid into a NaY zeolite, *Journal of Materials Science*. 46 (2011) 7511–7516. doi:10.1007/s10853-011-5722-2.
- [32] N. Salleh, U.S. Jais, S.H. Sarijo, Gelatin-coated zeolite y for controlled release of anticancer drug (zerumbone), in: *2012 IEEE Symposium on Business, Engineering and Industrial Applications (ISBEIA), 2012*: pp. 124–129. doi:10.1109/ISBEIA.2012.6422852.
- [33] M.P. Pina, R. Mallada, M. Arruebo, M. Urbiztondo, N. Navascués, O. de la Iglesia, et al., Zeolite films and membranes. Emerging applications, *Microporous and Mesoporous Materials*. 144 (2011) 19–27. doi:10.1016/j.micromeso.2010.12.003.
- [34] K.A. Fisher, K.D. Huddersman, M.J. Taylor, Comparison of micro- and mesoporous inorganic materials in the uptake and release of the drug model fluorescein and its analogues, *Chemistry*. 9 (2003) 5873–5878. doi:10.1002/chem.200304764.
- [35] A. Giaya, R.W. Thompson, R. Denkwicz Jr, Liquid and vapor phase adsorption of chlorinated volatile organic compounds on hydrophobic molecular sieves, *Microporous and Mesoporous Materials*. 40 (2000) 205–218. doi:10.1016/S1387-1811(00)00261-4.

- [36] K.B. Payne, T.M. Abdel-Fattah, Adsorption of Divalent Lead Ions by Zeolites and Activated Carbon: Effects of pH, Temperature, and Ionic Strength, *Journal of Environmental Science and Health, Part A*. 39 (2004) 2275–2291. doi:10.1081/ESE-200026265.
- [37] M. Spanakis, N. Bouropoulos, D. Theodoropoulos, L. Sygellou, S. Ewart, A.M. Moschovi, et al., Controlled release of 5-fluorouracil from microporous zeolites, *Nanomedicine: Nanotechnology, Biology and Medicine*. 10 (2014) 197–205. doi:10.1016/j.nano.2013.06.016.
- [38] A. Datt, E.A. Burns, N.A. Dhuna, S.C. Larsen, Loading and release of 5-fluorouracil from HY zeolites with varying SiO₂/Al₂O₃ ratios, *Microporous and Mesoporous Materials*. 167 (2013) 182–187. doi:10.1016/j.micromeso.2012.09.011.
- [39] N. Vilaça, R. Amorim, A.F. Machado, P. Parpot, M.F.R. Pereira, M. Sardo, et al., Potentiation of 5-fluorouracil encapsulated in zeolites as drug delivery systems for in vitro models of colorectal carcinoma, *Colloids and Surfaces B: Biointerfaces*. 112 (2013) 237–244. doi:10.1016/j.colsurfb.2013.07.042.
- [40] A. Datt, D. Fields, S.C. Larsen, An Experimental and Computational Study of the Loading and Release of Aspirin from Zeolite HY, *J. Phys. Chem. C*. 116 (2012) 21382–21390. doi:10.1021/jp3067266.
- [41] S. Grund, T. Doussineau, D. Fischer, G.J. Mohr, Mitoxantrone-loaded zeolite beta nanoparticles: Preparation, physico-chemical characterization and biological evaluation, *Journal of Colloid and Interface Science*. 365 (2012) 33–40. doi:10.1016/j.jcis.2011.09.003.
- [42] A. Nezamzadeh-Ejhieh, S. Tavakoli-Ghinani, Effect of a nano-sized natural clinoptilolite modified by the hexadecyltrimethyl ammonium surfactant on cephalexin drug delivery, *Comptes Rendus Chimie*. 17 (2014) 49–61. doi:10.1016/j.crci.2013.07.009.
- [43] M. Popova, A. Szegedi, V. Mavrodinova, N. Novak Tušar, J. Mihály, S. Klébert, et al., Preparation of resveratrol-loaded nanoporous silica materials with different structures, *Journal of Solid State Chemistry*. 219 (2014) 37–42. doi:10.1016/j.jssc.2014.07.002.
- [44] L.W. Wong, W.Q. Sun, N.W. Chan, W.Y. Lai, W.K. Leung, J.C. Tsang, et al., Zeolite microneedles for transdermal drug delivery, in: Z.G. Jiesheng Chen and Wenfu Yan Ruren Xu (Ed.), *Studies in Surface Science and Catalysis*, Elsevier, 2007: pp. 525–530.
- [45] S. Fox, T.S. Wilkinson, P.S. Wheatley, B. Xiao, R.E. Morris, A. Sutherland, et al., NO-loaded Zn²⁺-exchanged zeolite materials: A potential bifunctional anti-bacterial strategy, *Acta Biomaterialia*. 6 (2010) 1515–1521. doi:10.1016/j.actbio.2009.10.038.
- [46] D.A. LaVan, T. McGuire, R. Langer, Small-scale systems for in vivo drug delivery, *Nature Biotechnology*. 21 (2003) 1184–1191. doi:10.1038/nbt876.
- [47] R. Suedee, C. Bodhibukkana, N. Tangthong, C. Amnuait, S. Kaewnopparat, T. Srichana, Development of a reservoir-type transdermal enantioselective-controlled delivery system for racemic propranolol using a molecularly imprinted polymer composite membrane, *Journal of Controlled Release*. 129 (2008) 170–178. doi:10.1016/j.jconrel.2008.05.001.
- [48] S.A. Burns, J.A. Gardella Jr., Quantitative ToF-SIMS studies of protein drug release from biodegradable polymer drug delivery membranes, *Applied Surface Science*. 255 (2008) 1170–1173. doi:10.1016/j.apsusc.2008.05.082.
- [49] A.P.S. Immich, M.L. Arias, N. Carreras, R.L. Boemo, J.A. Tornero, Drug delivery systems using sandwich configurations of electrospun poly(lactic acid) nanofiber membranes and ibuprofen, *Materials Science and Engineering: C*. 33 (2013) 4002–4008. doi:10.1016/j.msec.2013.05.034.
- [50] L.G. Santos, D.C. Oliveira, M.S.L. Santos, L.M.G. Neves, F.O.G. de Gaspi, F.A.S. Mendonca, et al., Electrospun Membranes of Poly(Lactic Acid) (PLA) Used as Scaffold in Drug Delivery of Extract of *Sedum Dendroideum*, *Journal of Nanoscience and Nanotechnology*. 13 (2013) 4694–4702. doi:10.1166/jnn.2013.7194.
- [51] N. Uzun, T.D. Martins, G.M. Teixeira, N.L. Cunha, R.B. Oliveira, E.J. Nassar, et al., Poly(l-lactic acid) membranes: Absence of genotoxic hazard and potential for drug delivery, *Toxicology Letters*. 232 (2015) 513–518. doi:10.1016/j.toxlet.2014.11.032.

REFERENCES

- [52] W.B. Liechty, D.R. Kryscio, B.V. Slaughter, N.A. Peppas, *Polymers for Drug Delivery Systems*, *Annu Rev Chem Biomol Eng.* 1 (2010) 149–173. doi:10.1146/annurev-chembioeng-073009-100847.
- [53] H. Meng, J. Hu, A Brief Review of Stimulus-active Polymers Responsive to Thermal, Light, Magnetic, Electric, and Water/Solvent Stimuli, *Journal of Intelligent Material Systems and Structures.* 21 (2010) 859–885. doi:10.1177/1045389X10369718.
- [54] R. Cheng, F. Meng, C. Deng, H.-A. Klok, Z. Zhong, Dual and multi-stimuli responsive polymeric nanoparticles for programmed site-specific drug delivery, *Biomaterials.* 34 (2013) 3647–3657. doi:10.1016/j.biomaterials.2013.01.084.
- [55] W. Cheng, L. Gu, W. Ren, Y. Liu, Stimuli-responsive polymers for anti-cancer drug delivery, *Materials Science and Engineering: C.* 45 (2014) 600–608. doi:10.1016/j.msec.2014.05.050.
- [56] M. Zrínyi, Magnetic-field-sensitive polymer gels, *Trends in Polymer Science.* 5 (1997) 280–285.
- [57] S.G. Starodoubtsev, E.V. Saenko, A.R. Khokhlov, V.V. Volkov, K.A. Dembo, V.V. Klechkovskaya, et al., Poly(acrylamide) gels with embedded magnetite nanoparticles, *Microelectronic Engineering.* 69 (2003) 324–329. doi:10.1016/S0167-9317(03)00316-2.
- [58] Y. Deng, L. Wang, W. Yang, S. Fu, A. Elaissari, Preparation of magnetic polymeric particles via inverse microemulsion polymerization process, *Journal of Magnetism and Magnetic Materials.* 257 (2003) 69–78. doi:10.1016/S0304-8853(02)00987-3.
- [59] P. Tartaj, M. del P. Morales, S. Veintemillas-Verdaguer, T. González-Carreño, C.J. Serna, The preparation of magnetic nanoparticles for applications in biomedicine, *Journal of Physics D: Applied Physics.* 36 (2003) R182. doi:10.1088/0022-3727/36/13/202.
- [60] M. Babinová, D. Leszczynska, P. Sourivong, P. Čičmanec, P. Babinec, Superparamagnetic gel as a novel material for electromagnetically induced hyperthermia, *Journal of Magnetism and Magnetic Materials.* 225 (2001) 109–112. doi:10.1016/S0304-8853(00)01237-3.
- [61] M. Zrínyi, Intelligent polymer gels controlled by magnetic fields, *Colloid and Polymer Science.* 278 (2000) 98–103. doi:10.1007/s003960050017.
- [62] Q.A. Pankhurst, J. Connolly, S.K. Jones, J. Dobson, Applications of magnetic nanoparticles in biomedicine, *Journal of Physics D: Applied Physics.* 36 (2003) R167. doi:10.1088/0022-3727/36/13/201.
- [63] P. Martins, S. Lanceros-Méndez, Polymer-Based Magnetoelectric Materials, *Adv. Funct. Mater.* 23 (2013) 3371–3385. doi:10.1002/adfm.201202780.
- [64] G. Engdahl, C.B. Bright, Chapter 3 - Magnetostrictive Design, in: G. Engdahl (Ed.), *Handbook of Giant Magnetostrictive Materials*, Academic Press, San Diego, 2000: pp. 207–264.
- [65] A.R. Leach, *Molecular modelling: principles and applications*, 2nd Edition, Pearson Education Limited, 2001.
- [66] M. Alvaro, B. Ferrer, V. Fornés, H. García, J.C. Scaiano, Bipyridinium Macroring Encapsulated within Zeolite Y Supercages. Preparation and Intrazeolitic Photochemistry of a Common Electron Acceptor Component of Rotaxanes and Catenanes, *The Journal of Physical Chemistry B.* 106 (2002) 6815–6820. doi:10.1021/jp014088u.
- [67] D. Skoog, D. West, F. Holler, S. Crouch, *Fundamentals of Analytical Chemistry*, 9th ed., Cengage Learning, 2013.
- [68] Y.S. Nam, T.G. Park, Biodegradable polymeric microcellular foams by modified thermally induced phase separation method, *Biomaterials.* 20 (1999) 1783–1790. doi:10.1016/S0142-9612(99)00073-3.
- [69] T. Tanaka, D.R. Lloyd, Formation of poly(L-lactic acid) microfiltration membranes via thermally induced phase separation, *Journal of Membrane Science.* 238 (2004) 65–73. doi:10.1016/j.memsci.2004.03.020.
- [70] P. Martins, R. Gonçalves, A.C. Lopes, E. Venkata Ramana, S.K. Mendiratta, S. Lanceros-Mendez, Novel hybrid multifunctional magnetoelectric porous composite films, *Journal of Magnetism and Magnetic Materials.* 396 (2015) 237–241. doi:10.1016/j.jmmm.2015.08.041.
- [71] S. Dash, P.N. Murthy, L. Nath, P. Chowdhury, Kinetic modeling on drug release from controlled drug delivery systems, *Acta Poloniae Pharmaceutica.* 67 (2010) 217–223.

- [72] J. Siepmann, N.A. Peppas, Modeling of drug release from delivery systems based on hydroxypropyl methylcellulose (HPMC), *Advanced Drug Delivery Reviews*. 48 (2001) 139–157. doi:10.1016/S0169-409X(01)00112-0.
- [73] G. Arora, K. Malik, I. Singh, S. Arora, V. Rana, Formulation and evaluation of controlled release matrix mucoadhesive tablets of domperidone using *Salvia plebeian* gum, *Journal of Advanced Pharmaceutical Technology & Research*. 2 (2011) 163–169. doi:10.4103/2231-4040.85534.
- [74] L. Reimer, *Scanning Electron Microscopy: Physics of Image Formation and Microanalysis*, Springer Science & Business Media, 1998.
- [75] S.R. Matkovic, G.M. Valle, L.E. Briand, Quantitative analysis of ibuprofen in pharmaceutical formulations through FTIR spectroscopy, *Latin American Applied Research*. 35 (2005) 189–195.
- [76] E. Mendelovici, R. Villalba, A. Sagarzazu, O. Carias, The 1640 cm⁻¹ infrared band, monitor for the gain and thermal stability of water produced in ground kaolinites, *Clay Minerals*. 30 (1995) 307–313.
- [77] M. Ludvigsson, J. Lindgren, J. Tegenfeldt, FTIR study of water in cast Nafion films, *Electrochimica Acta*. 45 (2000) 2267–2271. doi:10.1016/S0013-4686(99)00438-7.
- [78] V. Sencadas, C.M. Costa, G. Botelho, C. Caparrós, C. Ribeiro, J.L. Gómez-Ribelles, et al., Thermal Properties of Electrospun Poly(Lactic Acid) Membranes, *Journal of Macromolecular Science, Part B*. 51 (2012) 411–424. doi:10.1080/00222348.2011.597325.
- [79] T. Hatakeyama, K. Nakamura, H. Hatakeyama, Determination of bound water content in polymers by DTA, DSC and TG, *Thermochimica Acta*. 123 (1988) 153–161. doi:10.1016/0040-6031(88)80018-2.
- [80] E.S. El-Leithy, D.S. Shaker, M.K. Ghorab, R.S. Abdel-Rashid, Optimization and characterization of diclofenac sodium microspheres prepared by a modified coacervation method, *Drug Discoveries & Therapeutics*. 4 (2010) 208–216.
- [81] P. Costa, J.M. Sousa Lobo, Modeling and comparison of dissolution profiles, *European Journal of Pharmaceutical Sciences: Official Journal of the European Federation for Pharmaceutical Sciences*. 13 (2001) 123–133.